

Coastal sand budget for Southern Pegasus Bay

Stage A

Prepared for Christchurch City Council

April 2018

Prepared by:

D M Hicks
R Gorman
R Measures
J Walsh
C Bosserelle

For any information regarding this report please contact:




Murray Hicks
Principal Scientist
River and Coastal Geomorphology

+64-3-343 7872

National Institute of Water & Atmospheric Research Ltd
PO Box 8602
Riccarton
Christchurch 8011

Phone +64 3 348 8987

NIWA CLIENT REPORT No: 2018062CH
Report date: April 2018
NIWA Project: CCC18501

Quality Assurance Statement		
	Reviewed by:	Emily Lane
	Formatting checked by:	Fenella Falconer
	Approved for release by:	Jo Hoyle

© All rights reserved. This publication may not be reproduced or copied in any form without the permission of the copyright owner(s). Such permission is only to be given in accordance with the terms of the client's contract with NIWA. This copyright extends to all forms of copying and any storage of material in any kind of information retrieval system.

Whilst NIWA has used all reasonable endeavours to ensure that the information contained in this document is accurate, NIWA does not give any express or implied warranty as to the completeness of the information contained herein, or that it will be suitable for any purpose(s) other than those specifically contemplated during the Project or agreed by NIWA and the Client.

Contents

- Executive summary 6**
- 1 Introduction 8**
 - 1.1 Background 8
 - 1.2 Scope of work 8
- 2 Methods..... 10**
 - 2.1 Waimakariri River supply of beach-grade sand 10
 - 2.2 Longshore transport rates 16
 - 2.3 Sand volume changes on Christchurch City beaches..... 18
 - 2.4 Sand exchange with the Avon-Heathcote Estuary 22
 - 2.5 Coastal sand budget compilation 23
- 3 Results 24**
 - 3.1 Waimakariri River supply of beach sediment 24
 - 3.2 Longshore transport rates 35
 - 3.3 Sand volume changes on Christchurch City beaches..... 42
 - 3.4 Sand exchanges with the Avon-Heathcote tidal deltas and estuary 47
 - 3.5 Coastal sediment budget 49
- 4 Conclusions 54**
- 5 Acknowledgements 55**
- 6 References..... 56**
- Appendix A Wave refraction modelling and longshore transport calculation..... 58**
- Appendix B ECan beach profile locations 61**
- Appendix C Starting offsets used in beach volume calculations 65**

Tables

- Table 2-1: Chainages at boundaries of littoral cells used by Tonkin & Taylor (2017) and this study. 21
- Table 3-1: Load-weighted average size gradings of measured suspended load and calculated total load for the 11-13 January 2018 Waimakariri River flood event and of the sampled bed material. 25

Table 3-2:	Sediment management practices at the main surface water takes from the Waimakariri River and tributaries.	30
Table 3-3:	Parameters influencing estimated annual sediment take at each major surface water take from the Waimakariri River.	31
Table 3-4:	Trap efficiency factors by size fraction for river sediment retention on beaches.	34
Table 3-5:	XBeach model results showing effect of counter-acting wind and current on wave-driven longshore transport.	42
Table 3-6:	Inner and outer profile closure depth estimates derived from Hallermeier's relations with the SWAN-modelled wave records for the period 2000-2017.	47
Table 3-7:	Estimated uncertainties on the beach sand budget components.	52

Figures

Figure 2-1:	Sampled Waimakariri flood of 11-13 January 2018.	11
Figure 2-2:	P-61 suspended sediment sampler deployed from jetboat on Waimakariri River.	12
Figure 2-3:	Suspended sediment rating curve for Waimakariri River at Old Highway Bridge.	13
Figure 2-4:	Suspended sediment rating data for Waimakariri, Rakaia, and Rangitata Rivers.	13
Figure 2-5:	Locations of ECan beach profile surveys over space and time for study shore.	19
Figure 2-6:	Concept sketch for an accreting beach profile.	21
Figure 3-1:	Size gradings of the total sediment load downstream of SH1 Bridge over 11-13 January 2018 flood.	24
Figure 3-2:	Frequency and cumulative distributions of the proportion of the long-term suspended load carried by different discharges.	25
Figure 3-3:	Proportion of the long-term suspended load carried by events with return period less than plotted value.	26
Figure 3-4:	Annual bulk volume sand loads of the Waimakariri River.	26
Figure 3-5:	Location of gravel extraction along lower Waimakariri River.	27
Figure 3-6:	Annual Waimakariri River gravel/sand extraction since 1960.	28
Figure 3-7:	Waimakariri River bed-material size grading.	29
Figure 3-8:	Brooklands Lagoon volume changes between 1932 and 1984.	32
Figure 3-9:	Size distributions of river suspended load, beach sand, and beach-trapping efficiency by size fraction.	35
Figure 3-10:	Alongshore distribution of mean annual northward, southward, net, and gross longshore sand transport, as predicted from SWAN wave modelling.	36
Figure 3-11:	Pegasus Bay bathymetry.	37
Figure 3-12:	Long-term average net longshore transport divergence.	38
Figure 3-13:	Daily longshore transport rates and time-cumulative longshore transport at Waimairi Beach (chainage 12.1 km).	39
Figure 3-14:	Cross-profile distribution of longshore transport simulated by XBeach model for different wave, wind, and externally-forced current scenarios.	41
Figure 3-15:	'Dispersion plot' showing space-time patterns of unit volume for backshore and foreshore combined.	43

Figure 3-16:	Trend rates for unit volume gain combined over backshore and foreshore at ECan profiles, 1990-2017.	44
Figure 3-17:	Average volumetric change rates in backshore and on foreshore within morphological cells.	45
Figure 3-18:	Trend rates for position of foredune toe and MSL line at ECan profiles, 1990-2017.	46
Figure 3-19:	Overlain trend rates for upper beach unit volume and average shoreline advance.	46
Figure 3-20:	Ebb-tidal delta seaward of the Avon-Heathcote Inlet.	48
Figure 3-21:	Bathymetric profile at Beatty Street, New Brighton.	49
Figure 3-22:	Beach volume budget components accumulated and totalled alongshore.	50

Executive summary

This report provides information on the contemporary coastal sediment budget of the Christchurch City beaches, between Taylors Mistake and the mouth of the Waimakariri River. A companion report will assess how this budget may change in the future. The work was commissioned by Christchurch City Council who will use the information to better understand how future changes in the coastal budget may affect coastal erosion and inundation extents, which in turn may influence floodplain and land-use management. The study results are to be fed into the multi-hazard analysis of the wider LDRP97 Project in preparing floodplain management plans. It is also anticipated that the project outputs will be used by Council's Land Drainage Team and Strategic Policy Unit to assist long term and regeneration planning.

The study tasks reported here include:

- Providing an updated estimate of the Waimakariri River's supply of beach-grade sand to the coast, including measuring the sand load of the river during a small flood.
- Estimating the wave-driven longshore transport potential along the study shore by undertaking a wave-refraction model study.
- Assessing changes in beach sand volume using the extensive beach-profile survey dataset compiled by Environment Canterbury.
- Assessing potential net sand exchanges with the Avon-Heathcote Estuary associated with the Christchurch Earthquake Sequence.
- Assembling the above components into a coastal sediment budget.

The main conclusions around the contemporary sand budget for the Christchurch City shore are:

- The Waimakariri River is the dominant beach sand source to the city shore, even though only about a quarter of its total sand load appears to be transported south and retained on the active beach profile along the city shore.
- Sand removed from the Waimakariri River channel during gravel extraction and at irrigation intakes is a minor fraction of its residual sand discharge to Pegasus Bay, and so has minimal impact on the coastal sand budget. Similarly, sand entrapment in Brooklands Lagoon also has minimal impact on the Waimakariri River's sand discharge.
- The river sand enters a bi-directional longshore transport system, with about 68% estimated to be moving southwards from the Waimakariri River mouth. For about 5-6 km south of the river mouth, processes other than wave-driven surf-zone longshore transport (e.g., transport by the river's discharge jet during floods) appear to be important in moving sand alongshore from the river mouth.
- Away from the river mouth area, wave-driven surf-zone transport would appear to be the dominant process responsible for transporting sand southward and for progressively depositing it due to a southward-waning transport capacity. A sensitivity analysis suggested that winds over the surf-zone and externally-forced currents (e.g., tidal currents and Canterbury Current eddies) appear to have minor net impact on the wave-driven transport.

- The city shore is accreting along most of its length, and the sand 'demand' to sustain this accretion must also prograde the lower beach profile, seaward of the MSL line out to the closure depth, as well as lift the beach profile to keep pace with rising sea-level. This total 'demand' for beach sand is more than twice the volume surveyed to be accumulating above the mean sea level line.
- Our estimate of this beach sand demand aligns reasonably well with our estimates of the supply of Waimakariri River sand to the city beaches. The sand budget misclose between supply and demand is well within the uncertainties accumulated from the various budget components.
- There is circumstantial evidence in the beach profile dataset that the Canterbury Earthquake Sequence, by altering the topography of the Avon-Heathcote Estuary and reducing its tidal prism, caused the estuary's ebb tidal delta to shrink, thus releasing sand to the adjacent beaches.

1 Introduction

1.1 Background

Christchurch City Council's (Council) Land Drainage Recovery Plan (LDRP) seeks to understand the post Canterbury Earthquake Sequence flood risk in the Greater Christchurch area by considering the influence of co-location, coincidence, and cascading of multi-hazards. Coastal erosion and inundation are two such hazards that link to other hazards, with their severity potentially affected by direct and indirect effects of earthquakes (e.g., shore uplift/subsidence, tsunami, landslide contributions to river sand delivery) and by rising sea level and changing wave-climate.

The coastal sediment budget is a key control on coastal erosion and inundation, but, as detailed in the LDRP113 Coastal Sediment Budget Study (Council 2017), there are knowledge gaps, or at least significant uncertainties, in components of the contemporary budget as well as how it might change in the future.

Accordingly, Council commissioned a study to provide updated information on the current coastal budget as well as better understanding of how future changes in this budget may affect coastal erosion and inundation extents, which in turn may influence floodplain and land-use management. The study results are to be fed into the multi-hazard analysis of the wider LDRP97 Project in preparing floodplain management plans. It is also anticipated that the project outputs will be used by Council's Land Drainage Team and Strategic Policy Unit in the course of long term and regeneration planning.

The study has been split into two stages:

- Stage A – updated sediment budget.
- Stage B - assessment of future sediment budget effects.

The objective of Stage A is to update the contemporary coastal sediment budget for the Christchurch beaches, including updating the supply of beach sand from the Waimakariri River, the longshore transport potential of waves incident on the Christchurch shore, and the sand volume stored in the beaches.

The Stage B objectives are to assess potential changes in the coastal budget due to climate change effects and a large earthquake affecting the Waimakariri catchment, and to assess the impact that any current or projected future changes in the coastal sediment budget would have on future shorelines, river mouth stability, and inundation hazards.

This report presents the results from Stage A, focussing on the contemporary coastal sediment budget.

1.2 Scope of work

The Stage A work scope included:

- Attending a workshop with relevant Council staff and the LDRP97 project team to confirm that the information to be provided by this study would meet the requirements of the analysis of multi-hazards and floodplain management options and to identify any further data gaps.

- Collating information and data pertaining to this study.
- Working with Council staff and stakeholders to understand their drivers.
- Developing an updated coastal sediment budget for Christchurch City beaches (Waimakariri River to Taylors Mistake) including an updated supply from the Waimakariri River, longshore transport, and beach volume.
- Assessing the influences on beach sediment delivery of gravel extraction and water abstraction from the Waimakariri River.

2 Methods

In overview, the Stage A workflow comprised five main tasks:

- Updating the estimate of the Waimakariri River's supply of beach-grade sand.
- Estimating the wave-driven longshore transport potential along the study shore.
- Assessing the changes in beach sand volume.
- Assessing potential net sand exchanges with the Avon-Heathcote Estuary.
- Assembling the results from the above components into a coastal sediment budget, including an assessment of component uncertainties.

In the following subsections we outline the methodologies associated with each of these tasks.

2.1 Waimakariri River supply of beach-grade sand

The objective was to determine the delivery of beach-grade sand to the Waimakariri River mouth while allowing for potential sand losses from the Waimakariri channel across the Canterbury Plains due to irrigation water abstraction, gravel extraction, and entrapment in Brooklands Lagoon. The key river sediment load measurement station, for which existing data on suspended sediment loads were available, is at the top of the tidal reach approximately at the SH1 bridge. Thus, the upstream irrigation takes and gravel extraction potentially reduce the sediment flux arriving at this point, while entrapment in Brooklands Lagoon will reduce the net flux delivered to the coast. A final consideration is how much of the river sand load remains in the shore zone.

2.1.1 Sediment load and size grading passing SH1 Bridge

Measuring total load and its size grading

No data on the size grading of the Waimakariri River's sediment load is available, nor has its total sediment load through the sand-bedded reach between SH1 Bridge and the coast been measured. Previously, estimates of the Waimakariri sand discharge to the coast have been made assuming a suspended load size grading matching that from several other larger Canterbury braided rivers reported by Hicks and Duncan (1993) and ignoring sand transport as bedload.

To fill this information gap, a series of sediment load measurements were made at a section some 2 km downstream of SH1 Bridge during a small flood peaking at 580 m³/s over 11-13 January 2018 (Figure 2-1). These measurements included six suspended sediment 'gaugings', each consisting of a discharge gauging followed immediately by collection of depth-integrated samples from five vertical profiles ('verticals') located at the centroids¹ of sub-sections of the river width carrying 20% of the total discharge. The discharge gaugings were done from the NIWA jetboat using an RDI Rio Grande Acoustic-Doppler Current-Profiler, with navigation by Differential GPS. The depth-integrated samples were collected with a 25 kg P-61 isokinetic sampler deployed from the jetboat (Figure 2-2). The samples from each vertical were composited for analysis of their mass concentration and size grading. The size grading was analysed by wet-sieving through 75 mm diameter sieves (0.063, 0.125, 0.25, 0.5, 1 mm mesh size). The masses of sediment caught on each sieve, and the mass of mud

¹ The centroid of a sub-section is the point across the sub-section width where 50% of the sub-section discharge is carried on each side of the point.

passing the sieve stack, were determined by filtering. These provided discharge-weighted suspended sediment concentrations by size grade.

The P-61 sampler only collects a sample to within 11 cm of the bed. The sediment load in the ‘un-sampled’ near-bed zone, moving as suspended load and bedload, was calculated using the ‘Modified Einstein Procedure’ using the US Bureau of Reclamation’s BORAMEP program (Holmquist-Johnson and Raff 2006). This uses the sampled suspended sediment size gradings and concentrations, the gauged velocities and depths, and the size-grading of the riverbed sediment. The riverbed sediment was sampled at the measurement section prior to the sampled flood using a BM-54 sampler to collect 6 evenly-spaced samples which were composited for size grading by dry sieving. The BORAMEP output provided total sediment load by size fraction.

A LISST-ABS near-field acoustic-backscatter sensor² was deployed over the sampled event from the bank near the measurement section, and its record was calibrated from the sediment gauging data to provide a continuous record of the suspended sediment concentration through the event (Figure 2-1). This was then combined with the discharge record from the Environment Canterbury (ECan) gauge at Old Highway Bridge (adjusted by ECan to remove tidal effects, lagged by approximately 30 minutes to allow for the travel time between the flow gauge and the sampling site, and adjusted to align the rated discharge with the gauged discharges) to calculate the sediment load over the event. The size gradings of the sediment load were interpolated between sampling times to provide an event-averaged size grading of the total load.

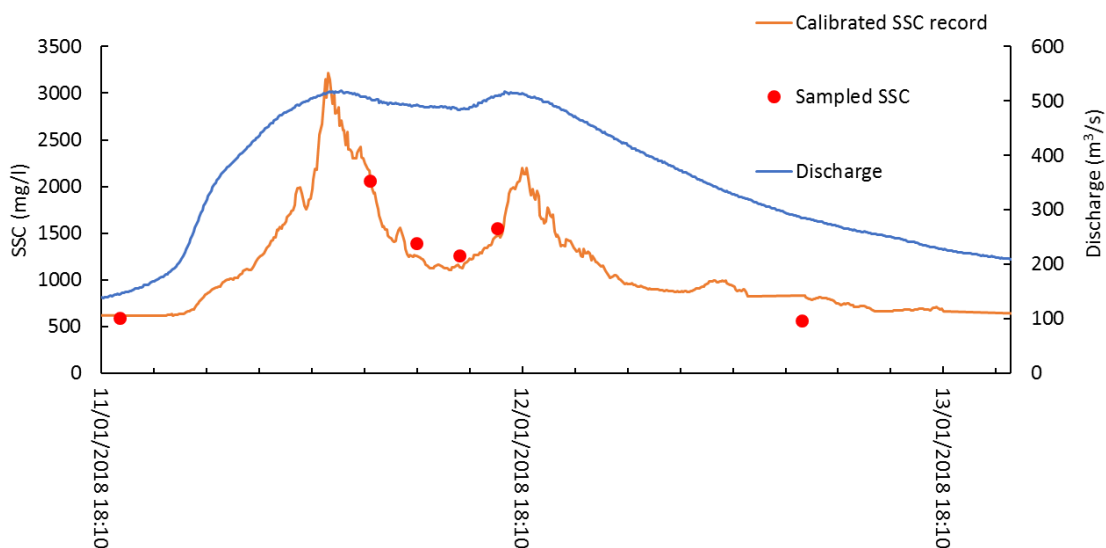


Figure 2-1: Sampled Waimakariri flood of 11-13 January 2018. SSC is discharge-weighted suspended sediment concentration. Orange line shows record derived after calibration of the LISST-ABS acoustic backscatter sensor.

² The LISST-ABS was used because its response is optimised for suspended sand, which is the focus of the study.



Figure 2-2: P-61 suspended sediment sampler deployed from jetboat on Waimakariri River.

Long-term average load and uncertainty

The long-term average suspended sediment load of the Waimakariri River past the SH1 bridge was determined by integrating the Old Highway Bridge (OHB) discharge record with a suspended sediment rating curve (i.e., the relationship between water discharge, Q , and suspended sediment concentration, C). This rating curve combined the six gaugings results from 11-13 January with 17 other gaugings collected at or around the OHB site by staff from the North Canterbury Catchment Board and/or Ministry of Works in the 1960s and 1970s (using depth-integrated sampling procedures similar to those used for this study). The 2018 data plotted in the same space as these older samples (Figure 2-3), confirming that the rating relationship has not changed since the 1960s-70s.

The rating curve was fitted using linear least-squares regression of log-transformed data, applying the estimator of Duan (1983) to correct for bias induced by the log transformation. The rating curve so derived is $C = 0.114Q^{1.552}$ where C has units of mg/s and Q units of m^3/s . The r^2 for this relation is 0.90 while the standard error of the estimate equates to multiplying or dividing the result by 1.8.

Comparison with similar sediment rating datasets from the Rakaia and Rangitata Rivers (Figure 2-4), both of which have more samples at lower flows compared to the Waimakariri River, indicated a steepening of the rating curve towards lower flows. We would expect similar from the Waimakariri River, so a low-flow range rating was created for the Waimakariri River to produce a similar trend. This estimates $C = 3.05E-7Q^{4.66}$ for $Q < 62 m^3/s$. The latter provides a (what would be barely visible) 8 mg/l concentration at $40 m^3/s$ compared to 35 mg/l with the original rating. The impact of this modification on the long-term average load is trivial (<0.3%).

The uncertainty on the long-term average load associated with the scatter on the rating curve was found by using the standard error of the rating to estimate the standard error associated with the load carried by each flow band. The root-sum-of-variance across all flow bands provides a standard error estimate for the long-term average load. This was found to be $\pm 6.5\%$. The 95% confidence interval was $\pm 19.8\%$.

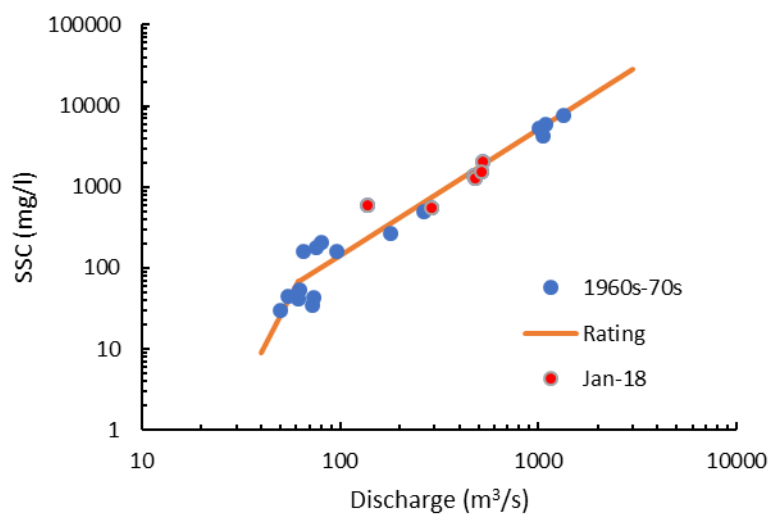


Figure 2-3: Suspended sediment rating curve for Waimakariri River at Old Highway Bridge. SSC is suspended sediment concentration (C in text). Blue points show data collected in 1960s-70s; red points are data collected for this study in January 2018. Longer orange line shows regression-fitted rating curve. The shorter, steeper segment was fitted to align with the pattern shown by Rakaia and Rangitata Rivers (Figure 2-4). Discharge is Q in text.

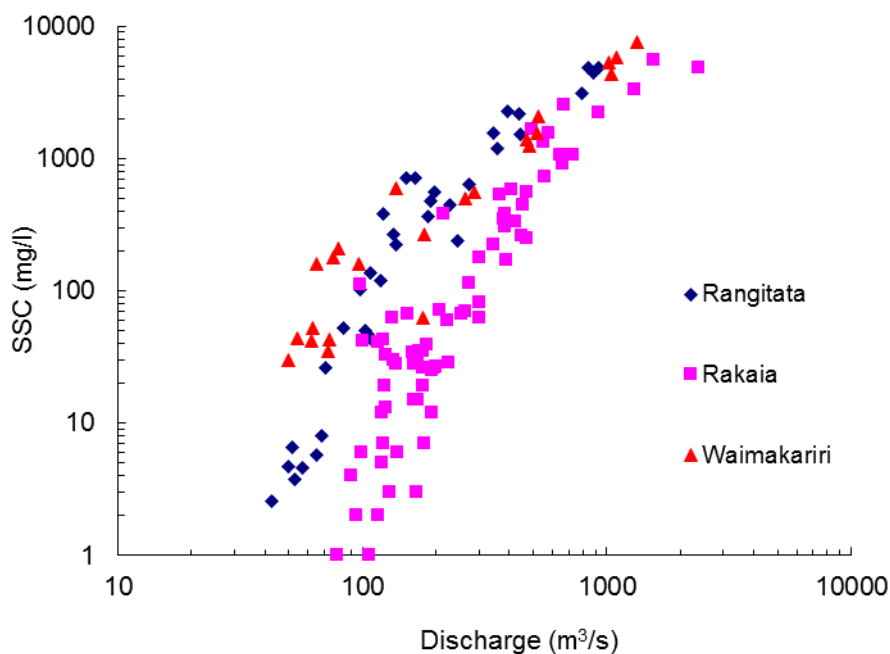


Figure 2-4: Suspended sediment rating data for Waimakariri, Rakaia, and Rangitata Rivers. SSC is suspended sediment concentration. Note curve steepening towards lower flows for Rakaia and Rangitata Rivers.

Load distribution by flow

The proportion of the total long-term average load carried by each 10-m³/s flow band across the flow range (40-2910 m³/s) was determined by combining the suspended sediment rating curve with a flow-distribution table extracted from OHB flow record.

A ‘partial-duration’ series approach was used to determine the load carried by floods of given return period. This involved integrating the sediment load over discrete events, then assigning return periods to the ranked results using a simple $T = n/m$ ‘plotting formula’ (where n is the number of years of record and m is the event rank). A hydrograph separation slope of 0.00007 m³/s², fitted by inspection, was used to identify the start and finish of high flow events.

Load variability

Annual variability in the Waimakariri River’s sand load was determined by integrating the suspended sediment load on a year-by-year basis, then adjusting the annual loads to sand equivalent loads assuming a constant size grading.

2.1.2 Sand removed with gravel extraction

Gravel is extracted from the bed of the lower Waimakariri River to prevent bed aggradation, which would otherwise increase flood risk, and to supply gravel and sand for roading and construction. While the Waimakariri River does not have the competence to transport its gravel bedload to the coast along its low gradient tidal reach, the question has been raised as to whether sand extracted with the gravel would otherwise be delivered to the coast.

This was addressed by:

- Collating and analysing data on volumetric gravel extraction rates from ECan reports.
- Collating data on size gradings of bed-material from the lower Waimakariri River channel and assessing the bed material sand content. These data were available from our own measurements (collected for research projects), an historical dataset collected by the North Canterbury Catchment Board, and from size gradings of samples from gravel stockpiles obtained from the gravel extraction industry.

2.1.3 Sand removed by irrigation water abstraction

A portion of the Waimakariri River’s sand load delivered from the mountains is extracted with irrigation water. To assess the impact of this on the coastal sand supply, we assessed: (i) how much sand load is drawn into irrigation canals during freshes, and (ii) how much of this is intercepted by settling ponds and returned periodically to the river. The sand load withdrawal was estimated by combining water take rates with the Waimakariri River suspended sediment rating (Figure 2-3), assuming the same sand proportion of the suspended load as measured in Section 2.1.1. Information on rates of water take and sand returns to the river were obtained by interviews with the main water extractors.

2.1.4 Entrapment downstream of SH1, particularly in Brooklands Lagoon

Before 1940, the Waimakariri River discharged into Pegasus Bay through Brooklands Lagoon, looping into the Lagoon from the north. In 1930, a cut had been made in the sand hills to create a direct course to the sea for the Waimakariri River to reduce flooding, but the river continued to use its natural mouth until 1940 when a flood forced the river into the new northern outlet (Boyle 2011). Since then, Brooklands Lagoon has been a “dead arm”, trapping sediment from Waimakariri River

floods and sand blown or washed over the Brooklands Spit from the ocean beach. It has thus been a “sink” for some of the Waimakariri River’s sediment load. We assessed the size of this diversion by reviewing existing reports.

We assumed that the Waimakariri River channel between SH1 Bridge and the contemporary mouth at Kairaki is neither trapping sand nor eroding but is in a state of dynamic equilibrium on a long-term average basis, thus it has no impact on the coastal sediment budget. This assumption is based on a lack of issues relating to ongoing sediment accumulation or scour. While there have been localised transient channel engineering issues relating to bank erosion and bar growth (Tony Boyle, ECan, pers comm.), there would appear to be no trends for increasing or decreasing channel volume. Similarly, erosion and sand bar growth at the spit tip on the south side of the river mouth appear to be short term processes (Boyle 2011).

2.1.5 Proportion of river load retained on shore

Not all the Waimakariri River’s sediment load discharged to Pegasus Bay is retained on the adjacent beaches and so contributes to the beach sediment budget. This is quite clear from the literature on seabed sediment composition in Pegasus Bay, which shows a gradual seaward progression from sand on the beach face to a mixture of progressively more mud and progressively finer sand (e.g., Carter and Herzer 1986, Allan et al. 1999).

To assess the proportion that is retained, we estimated the trap efficiency of the different size fractions of the its total sediment load. This was done by trial-and-error alignment of the size grading of the river load (determined as in Section 2.1.1), weighted by trap efficiency, with representative beach sediment size gradings derived from existing datasets.

Three beach size-grading datasets were used:

- The data of Blake (1967). Blake reported foreshore sand gradings of samples from 12 sites between the Avon-Heathcote Estuary and the Waimakariri River mouth. These were processed to provide a spatially-averaged size grading. Grainsize percentiles were derived by inverting the published statistics (i.e., mean, median, sorting skewness, etc).
- ECan data (Justin Cope, pers. comm.). Sand samples were collected by ECan in 1997 from a sub-set of their regularly-monitored profiles between Sumner and the Waimakariri River mouth. These comprised 38 mid-tide sites, 12 upper-foreshore sites, and 7 foredune sites. The average size distributions of the mid-tide, upper-foreshore, and foredune data were combined into a simple average size distribution representing the foreshore. The dataset included grainsize percentiles.
- The data of Allan et al. (1999). Allan et al. reported size-grading data for 17 samples collected across the entire beach profile at Bridge Street, including the foreshore (above mean low water level) and the nearshore out to a depth of 14 m (below MSL), some 2300 m offshore. Grainsize percentiles as a function of distance offshore were extracted from the cross-shore functions for mean size, sorting, and skewness provided by Allan et al.

The Blake (1967) and ECan data provide good representativeness alongshore, but are only for the foreshore – whereas the full extent of the beach extends to its closure depth in the nearshore. Since foreshore sand sizes are generally expected to be coarser than those in the nearshore, the Blake and ECan data may be coarser than a sample representative of the full width of profile. The Allan et al.

(1999) dataset does cover the full width of beach but is only for one site – so it also may not be representative of the study shore overall.

2.2 Longshore transport rates

Wave-driven longshore transport rates along the study shore were estimated by combining records of refracted waves with a longshore-transport formula. The refracted wave records were based on the deep-water wave record collected by the wave buoy off Steep Head, Banks Peninsula from August 2000 through December 2017.

Since the longshore current associated with longshore sand transport may also be influenced by winds, tide, and shelf currents, we also undertook a sensitivity study to assess the significance of ignoring these other current drivers.

2.2.1 Wave refraction with SWAN model

Wave conditions along the project coast for the period 1 September 2000 through 31 December 2017 were simulated using the SWAN (Simulating Waves Nearshore) model using the Banks Peninsula wave buoy record and an assumed spatially uniform inshore wind record as boundary conditions. Details of the SWAN model are provided in Appendix A. The SWAN model was run in full spectral mode on NIWA's high performance Cray XC50 'supercomputer', and, owing to the large model domain, 1 km grid size, and 30-minute records, it required almost four days of run-time to process the approximately 17 years of data.

The Banks Peninsula wave buoy site is exposed to persistent southerly swells which are largely blocked by Banks Peninsula from reaching the Pegasus Bay coast. On the other hand, waves from the eastern quadrant have a relatively stronger impact at the Pegasus Bay coast than at the buoy location. Being more locally-generated, these will generally occur in the buoy record at higher frequencies than the southerly swell. Where both are present simultaneously, the spectral formulation in SWAN used herein will allow for both components of the sea state to be satisfactorily represented. In the Gorman et al. (2002) study, by contrast, it was only possible to apply parametric boundary conditions, specifying a single mean direction and directional spread to apply to all frequencies. Hence only one component could be represented at a time, meaning that the role of waves reaching Pegasus Bay from the northeast could often be under-represented relative to those from the southeast. Gorman et al. (2002) noted that their study indicated net northward longshore transport potential all along Pegasus Bay, whereas the general appreciation is that there is net southward transport from the Waimakariri River – which is necessary to account for the prograding shoreline.

Outputs from the SWAN simulations were extracted at a set of points spaced some 700-800 m apart along the 10-m isobath, and were then transformed to the wave break point assuming approximately shore-parallel contours shoreward of the 10-m isobath (as detailed in Appendix A). A key output was the longshore flux factor (i.e., the flux per m length of shore of longshore directed wave energy across a shore-parallel line), P_{ls} (watts/m), which was the 'driver' of the longshore transport formula used.

2.2.2 Longshore transport model

We chose the relatively simple 'CERC' empirical wave-driven longshore transport formula to calculate longshore transport rates. This relates the surf-zone longshore sediment flux Q (bulk m^3/yr) to the longshore flux factor P_{ls} :

$$Q = fKP_{ls} \quad (1)$$

where $f = 3259 \text{ m}^2\text{s}^3/\text{kg}/\text{yr}$ is a unit-conversion constant, while K is a dimensionless efficiency factor dependent on sediment properties.

Using a significant wave-height formulation, K has been found to take a value of 0.39 for dissipative sandy beaches similar to those in Pegasus Bay (CERC 1985). In this study, we calibrated K to a value of 0.21 to align with other sand budget information (as detailed in Sections 3.2.3 and 3.5.2 below). For this study, we use the convention that northward transport has positive values.

We accumulated the northward longshore transport (Q_n) and southward longshore transport (Q_s) separately at each wave output point. The net transport (Q_{net}) equals $\sum Q_n - \sum Q_s$, while the gross transport (Q_{gross}) equals $\sum Q_n + \sum Q_s$. $\sum Q_s/Q_{gross}$ indicates the proportion of the gross transport directed south.

Longshore transport across the boundaries of the eight beach cells (A-G) defined by Tonkin & Taylor (2017) was found by interpolating between the nearest SWAN output stations.

2.2.3 Importance of other current drivers – Sensitivity analysis

The above formulation assumes that all significant long-shore transport occurs in the surf-zone and is driven by obliquely-approaching breaking waves. This ignores the effects of nearshore longshore currents forced by the tide, local wind, and shelf-scale oceanic currents (, the anti-clockwise eddy in Pegasus Bay that is ‘spun-up’ by the northward-moving Canterbury Current in the wake of Banks Peninsula) - both outside the surf-zone under unbroken waves, and inside the surf-zone where the net longshore current could potentially be in the opposite direction to that forced only by longshore-directed wave momentum.

A fully specified longshore transport model capturing all potential longshore transport drivers (i.e., wind, tide, and oceanic currents as well as waves) is beyond the scope of this study; indeed, it would require coupling to a calibrated shelf-scale hydrodynamic model for which there are no boundary condition data available for the past 17 years to match the wave buoy record. However, we did assess the potential sensitivity to other longshore-current drivers using the XBeach model with simplified input parameters.

The XBeach model (Roelvink et al. 2009) provides a full hydrodynamic solution to shore processes. A simple model was set up on a 5-m grid spanning 4.2 km of shore and extending 2.1 km seaward to the 16-m depth contour, using a representative profile of the Christchurch city shore and assuming parallel contours to create the bathymetry. The seabed was stocked with sand of 0.2 mm median diameter and 0.28 mm D_{90} (from the data of Blake 1967) and a density of $2650 \text{ kg}/\text{m}^3$. The model was forced by a wave condition typical of that experienced on the Christchurch shore: a JONSWAP wave spectra with a significant wave height of 1.0 m, peak period of 10 s, and a peak direction from due East (with a directional spread of 800 and a peak enhancement factor of 3), arriving with a 13-degree approach angle to a shore oriented 13 degrees West of North (and so driving a northward longshore current and sand transport). The Soulsby-van Rijn (Soulsby 1997, van Rijn 1985) sediment transport formulation was used. With this basic set-up, five scenarios were run to assess the effects on the wave-driven longshore transport of an opposing north-easterly wind and a south-setting tidal or shelf current:

1. No wind and no longshore currents (only waves).
2. Waves plus a 5 m/s north-east wind (representing average wind conditions), no shelf current.
3. Waves plus a 15 m/s north-east wind (representing maximum wind conditions), no shelf current.
4. Waves, a 0.2 m/s southward current (representing common current conditions), no wind.
5. Waves, a 0.7 m/s southward current (representing peak current conditions), no wind.

A wind drag coefficient³ of 0.002 was applied for the scenarios with wind forcing, and the wind field was assumed to be uniform over the model domain.

The cross-shore distribution of longshore transport magnitude and direction and the net transport integrated over the nearshore were extracted from the XBeach model for each scenario. Since no model calibration was undertaken, the results must be regarded as indicative only.

2.3 Sand volume changes on Christchurch City beaches

The net gain (or loss) of sand volume on the city's beaches surveyed by ECan's beach profile network provides a partial measure of whether the beach budget is in surplus or deficit. However, the ECan surveys only cover the subaerial beach (backshore-foreshore), not the submerged, nearshore 'foundation' of the beach, which must be considered in a full accounting of beach sand volume.

Therefore, our assessment of sand retention on the study beaches includes:

- Analysing sand volume changes in the foreshore-backshore out to and above the MSL contour (hereafter termed the "upper beach") from ECan's profile survey dataset.
- Estimating the depth of the effective seaward limit, or closure depth, of the nearshore segment of the beach profile (termed the "lower beach"), and assuming that sand volume changes on the lower beach would occur in proportion to those on the upper beach.

2.3.1 Upper beach volume changes off beach profile data

ECan has surveyed a network of beach profiles along the Canterbury coast on semi-annual to annual basis since 1990. This network has 46 profiles along the study shore between Taylors Mistake and the south side of the Waimakariri River mouth (Gabites 2005). These profile locations are mapped in Appendix B. The profiles along the Christchurch City shore are labelled by ECan based on their distance (or "chainage") northward alongshore from a reference point at Sumner Head⁴ (e.g., Profile C1130 is located 11.30 km north of Sumner Head). For simplicity, we also referenced the Taylors Mistake profile chainages relative to this point.

The locations of surveys along the study shore over space and time are shown on Figure 2-5. Typically, these have been survey twice-yearly, nominally in summer and winter, although sometimes

³ This is the drag coefficient C_d that is used to predict wind stress on the sea surface (τ_w) from the equation $\tau_w = \rho_a C_d U_w^2$, where ρ_a is density of air and U_w is wind velocity.

⁴ Although the exact location of this reference point at Sumner Head is not provided by Gabites (2005), we estimate its NZTM location to be approximately 1581881E and 5175344N.

only once per year. The span of shore represented by individual profiles ranges from 40 m (near the New Brighton Pier) to 1775 m (Bottle Lake area) and averages 507 m. The latest data supplied were from the August-October 2017 survey.

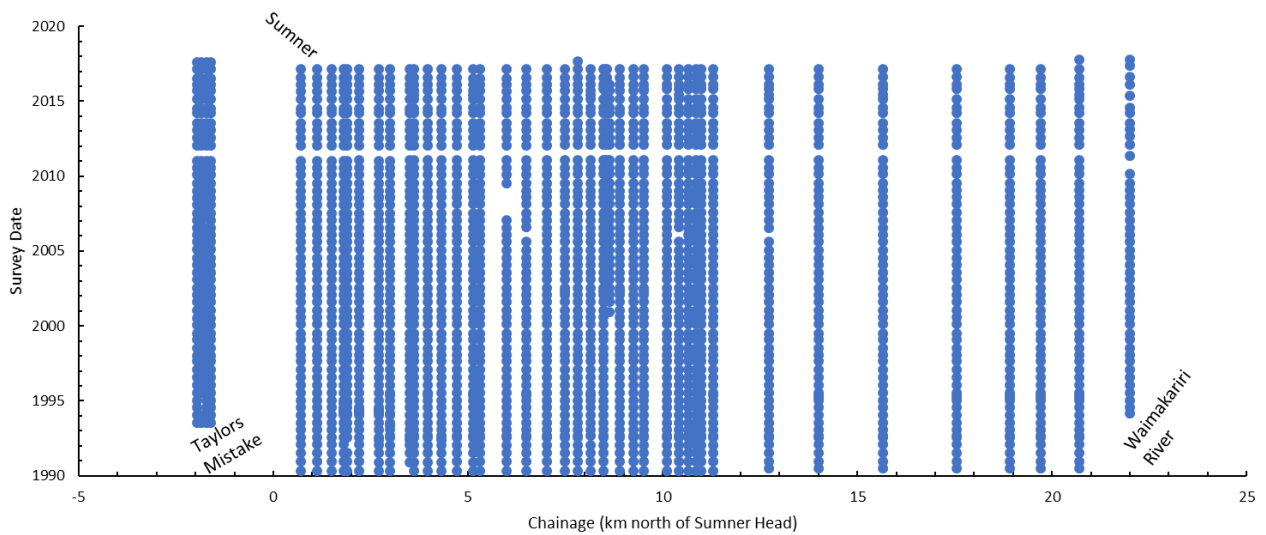


Figure 2-5: Locations of ECan beach profile surveys over space and time for study shore.

The profile data are archived by ECan using the Beach Profile Analysis Toolbox (BPAT). The data were supplied by ECan as text files exported by BPAT, and these were re-loaded into BPAT for our analysis. Data preparation included the following steps:

- Identifying the landward offset from which to begin beach volume calculations. The landward ends of surveys at a particular profile varied due to the field surveyor judging that the backshore profile had not changed significantly since the previous full backshore survey and hence not surveying the backshore profile all the way to the benchmark. Moreover, there was inconsistency in the choice of the landward end-point from one survey to the next. Data preparation to manage these issues comprised: (i) infilling missing backshore data using BPAT templates, with template data set from the previous full backshore survey; and (ii) choosing a common end-point applicable to all surveys of the profile. For most profiles a reliable end-point that fully captured the change in backshore volume over time could be assigned. However, some profiles had data that was too sparse in the backshore and required an end-point to be assigned that was further seaward than ideal to avoid spurious inter-survey volume changes. This means that the backshore beach volume changes for those profiles may not have been fully captured. The offsets to the volume-calculation end-points for each profile are listed in Appendix C, along with an assessment of how well the backshore volume change was assessed.

- Tagging points at the foredune toe, where these had not already been tagged from the field surveys⁵. We deemed the foredune toe to mark the boundary between the backshore and foreshore, which enabled a separate calculation of backshore and foreshore volume change. An algorithm was trained to automatically detect the foredune toe location based on the expected elevation range and change in profile gradient. Checks against the field-tagged foredune toe location confirmed this approach to be reliable.

Data analysis involved:

- Calculating unit sand volumes (m³ per m length of beach) above the MSL datum for the backshore and foreshore segments of the profile (integrating the 'area' under the profile between the stable backshore, foredune toe, and MSL line offsets).
- Calculating time trends in unit volume gain or loss at each profile using linear regression, using all surveys between 1990 and 2017.
- Calculating time trends in the offset of the foredune toe and MSL line, using all surveys between 1990 and 2017.
- Plotting 'dispersion' diagrams, which show the space-time pattern of profile volume change (e.g. Figure 3-15). These plots were prepared within the SURFER geospatial software package by gridding the unit volume deviations from the time-averaged unit volume across time and space for every survey. The gridding used linear interpolation with Delauney triangulation, with 0.25 yr time intervals and 0.5 km longshore intervals.
- Accumulating the volume change alongshore by weighting the unit volumes at each profile by the span of shore represented by each profile (equal to half the distance between the two adjacent profiles), and then accumulating volumes alongshore.
- Extracting the volume changes within the eight littoral cells, A-G, used by Tonkin & Taylor (2017). This was done by weighting the profile unit volume changes by their spans lying within the Tonkin & Taylor littoral cells. Table 2-1 lists the longshore chainages defining the boundaries of Tonkin & Taylor's (2017) littoral cells and their equivalent chainages in the ECan system used in this study. Tonkin & Taylor chainages (*T&T*, km) can be converted to the ECan chainages (*ECan*, km) used in this study with the relation: $ECan = 12.16 - T\&T$. Since Tonkin & Taylor only defined eight cells for the span of shore between Waimairi Beach and South Shore, we defined three additional cells (Bottle Lake South, Bottle lake North, and Brooklands) between Waimairi Beach and the Waimakariri River mouth, and two cells (Sumner and Taylors Mistake) to the south of South Shore (Table 2-1).

⁵ Gabites (2005) appears to use the term "beach toe" for what we term the foredune toe – we find this use of "beach toe" confusing and have avoided it.

Table 2-1: Chainages at boundaries of littoral cells used by Tonkin & Taylor (2017) and this study. All chainages in km. This study uses ECan chainages. Tonkin & Taylor cells A-G chainages defined in Table 4-3 of Tonkin & Taylor (2017).

Cell	T&T chainage N end	T&T chainage S end	ECan chainage N end	ECan chainage S end
Brooklands			22.00	17.55
Bottle Lake N			17.55	14.00
Bottle Lake S			14.00	12.16
A	0	1.95	12.16	10.21
B	1.95	3.7	10.21	8.46
C	3.7	5.2	8.46	6.96
D	5.2	6.3	6.96	5.86
E	6.3	7.25	5.86	4.91
F	7.25	8.65	4.91	3.51
G	8.65	9.6	3.51	2.56
Sumner			2.21	0.70
Taylor's Mistake			-1.60	-1.95

2.3.2 Estimating lower beach volume changes

In the absence of repeat nearshore surveys to match ECan's beach surveys, volume changes on the lower part of the beach profile (seaward of MSL line out to the closure point) were estimated based on the assumption that the full profile should advance or retreat in parallel, without any change in profile shape. Thus, the ratio of volume change on the upper profile to volume change on the lower profile should match the ratio of upper beach height (H) to closure depth (D_c) – as shown conceptually in Figure 2-6.

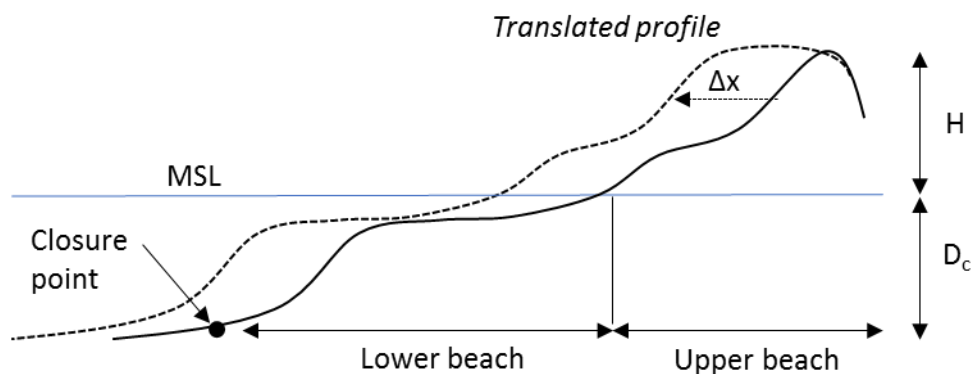


Figure 2-6: Concept sketch for an accreting beach profile. The upper and lower segments of the profile advance in parallel, with total volume change (per unit shore length) equal to $(H + D_c) \cdot \Delta x$, where Δx is the seaward advance.

The assumption stems from the fact that beach profiles tend to fit an equilibrium profile matched to the incident wave climate and beach sediment stock (Bruun 1954). Beach profile shape, although naturally quite variable and affected by various factors (e.g. storms, swell, rip currents, bar systems),

on a long-term average basis tends to fit an equation of the type $h(y) = Ay^{2/3}$, where y is the distance from the shoreline, $h(y)$ is the profile depth, and A is a parameter depending mainly on wave energy and sediment grainsize⁶. Therefore, if the wave climate and sediment size remain unchanged, any surplus or deficit in the sediment budget should translate the beach profile seaward or landward but not change its shape. The assumption is widely employed in coastal engineering applications, including the “Bruun rule” that predicts beach profile response to sea-level rise (Bruun 1962), design of beach nourishment sand volume requirements (Dean 1991), and “1-line” shoreline morphodynamic modelling (e.g. Hicks 1993).

We estimated the depth of the profile closure point using much the same approach as used by Tonkin & Taylor (2017) for their assessment of shore retreat associated with sea level rise. This considered inner and outer limit depths (D_i and D_o) based on the Hallermeier’s relations (as reported by Nicholls et al. 1998):

$$D_i = 2.28 H_{s,t} - 68.5 H_{s,t}^2 / gT_s^2 \quad (2)$$

and

$$D_o = 1.5D_i \quad (3)$$

where D_i and D_o are depths (m) below Mean Low Water Springs, $H_{s,t}$ is the non-breaking significant wave height (m) exceeded for $t = 12$ hours per year on average, and T_s (s) is the associated wave period. We derived values for D_i and D_o by analysing the approximately 17-years of hourly records of significant wave height output from the SWAN model at the 10-m contour along the study shore. We increased the D_i and D_o values so derived by 1 m to convert them to depths below MSL.

We note that this approach for determining closure depth differs from the approach used by Tonkin & Taylor (2017) in that while we used refracted and shoaled wave records generated at the study shore, Tonkin & Taylor appear to have simply used the records measured in deep water at the Banks Peninsula wave buoy. We consider that use of the more energetic wave conditions at the buoy site will overestimate the depth limits along the relatively sheltered city shore.

2.4 Sand exchange with the Avon-Heathcote Estuary

The Avon-Heathcote Inlet and Estuary, including the inlet’s ebb and flood tidal deltas, represent a potential source or sink for the beach sand on the open coast.

We considered possible permanent sand exchanges between the beach system and the ebb- and flood-tidal deltas of the Avon-Heathcote Estuary by considering tidal prism changes following the Christchurch Earthquake sequence, in the context of Hicks and Hume’s (1996) empirical relation between ebb tidal delta volume (V , m³) and spring tidal prism (P , m³):

$$V = 1.37 \times 10^{-3} P^{1.32} (\sin\vartheta)^{1.33} \quad (4)$$

where ϑ is the angle between the ebb-flow and the adjacent shoreline.

Partial derivatives of this equation provide the following proportional estimator of change in ebb delta sand volume:

⁶ On the City shore, bathymetry profiles at Beatty Street from Allan et al (1999), shown in Figure 3-21 of this report, fit this equilibrium beach profile equation with a value for 0.07 – 0.08 for the A parameter.

$$dV/V = 1.32 dP/P \quad (5)$$

where dV and dP are relatively small changes in the original values of the delta sand volume and tidal prism, V and P . Thus, for example, a 10% increase in tidal prism would result in a 13.2% increase in ebb delta volume, which would require sand being drawn from the adjacent beaches.

2.5 Coastal sand budget compilation

The results from the above tasks were compiled into a sand budget for the study shore. This included adjusting the transport efficiency factor, K , in the longshore transport relation to align wave-driven surf-zone transport with observed sand volume changes.

3 Results

3.1 Waimakariri River supply of beach sediment

3.1.1 Total load passing SH1 Bridge and its size grading

Using the Modified Einstein Procedure to calculate the total sediment load for each of the six sediment gaugings from the 11-13 January 2018 flood event, we found that the load-weighted event-averaged total load comprised 85.3% measured suspended load and 14.7% unmeasured load (i.e., sand moving as suspended or bed load in the near-bed un-sampled zone).

Figure 3-1 shows that the size gradings of each of the six measurements of the total load were reasonably consistent (total sand content 26%-36%, except for a higher sand content of 53% for Gauging G6 taken during the flood recession on 13 January). The load-weighted total load size grading averaged over all gaugings is listed in Table 3-1. This is the grading assigned to the delivery of sand at the river mouth. It shows that the load-weighted average sand proportion of the total load was 33.5%.

The total sand load over the event equated to 39.4% of the measured suspended load over the event. This is the figure that should be applied to derive the long-term average sand load when using the Waimakariri River at OHB suspended sediment rating curve, since the rating curve data are based only on the measured suspended load not the total load.

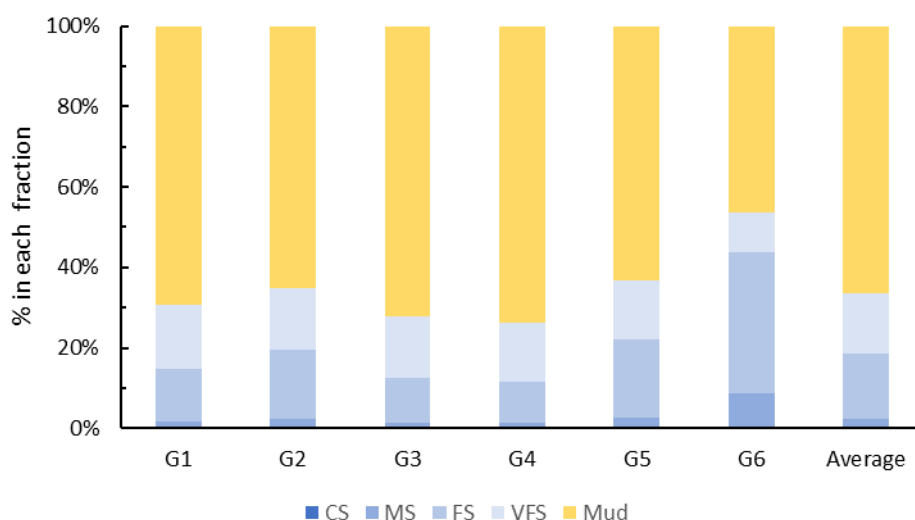


Figure 3-1: Size gradings of the total sediment load downstream of SH1 Bridge over 11-13 January 2018 flood. G1-G6 show results for separate gaugings. The average of all gaugings is plotted on the right. CS = coarse sand (0.5-1 mm); MS = medium sand (0.25-0.5 mm); FS = fine sand (0.125-0.25 mm); VF = very fine sand (0.063-0.125 mm); Mud = silt and clay (< 0.063 mm). The average sand proportion is 33.5%.

Table 3-1: Load-weighted average size gradings of measured suspended load and calculated total load for the 11-13 January 2018 Waimakariri River flood event and of the sampled bed material. Values show % by mass in each size interval.

Grainsize fraction	Measured suspended load	Calculated total load	Average of bed-material samples
Coarse sand (0.5-1 mm)	0.29%	0.03%	0.26%
Medium sand (0.25-0.5 mm)	0.58%	2.42%	15.10%
Fine sand (0.125-0.25 mm)	7.33%	16.25%	67.90%
Very fine sand (0.063-0.125 mm)	13.41%	14.75%	10.48%
Mud (< 0.063 mm)	78.38%	66.55%	6.26%

Long-term average suspended load and sand load of the Waimakariri River

By combining the Waimakariri River suspended sediment rating curve derived in Section 2.1 with the Waimakariri River discharge record from 1 January 1967 through 1 November 2017 (almost 51 years), the long-term average suspended load was found to be 3.03 million t/yr (with a standard error of 6.5%). Using the above sand proportion results, the long-term average sand load is therefore $3.03 \times 0.394 = 1.19$ million t/yr. Assuming a sand bulk density of 1.6 t/m^3 , this equates to a volumetric sand discharge of $746,000 \text{ m}^3/\text{yr}$.

Load distribution by flow

Figure 3-2 shows the proportion of the total long-term average Waimakariri River suspended load carried by each $10\text{-m}^3/\text{s}$ band across the flow range ($40\text{-}2910 \text{ m}^3/\text{s}$). This shows that the load is distributed over a broad range of flows but with the more common midrange flows carrying more than the very high flows. 77.4% of the load is carried at flows between the mean ($119 \text{ m}^3/\text{s}$) and the mean annual flood ($1495 \text{ m}^3/\text{s}$).

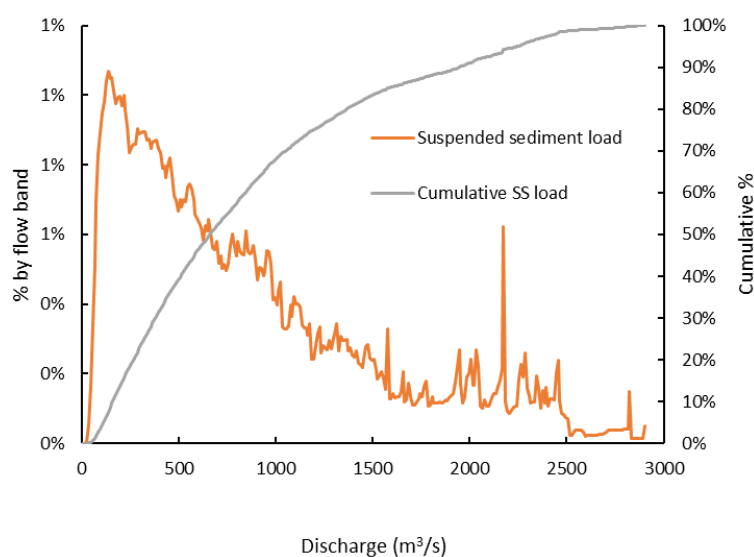


Figure 3-2: Frequency and cumulative distributions of the proportion of the long-term suspended load carried by different discharges. The discharge range is banded into $10 \text{ m}^3/\text{s}$ intervals.

Similarly, Figure 3-3 shows that 48% of the long-term load is transported by events with a recurrence interval of one year or less, while only 8.6% is transported by events with recurrence intervals exceeding 20 years. Thus, it is the relatively common freshes and floods that transport the bulk of the Waimakariri River’s suspended load.

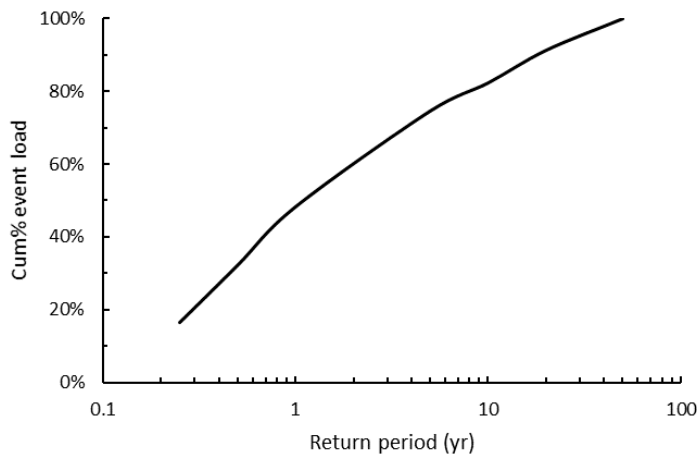


Figure 3-3: Proportion of the long-term suspended load carried by events with return period less than plotted value.

Load variability

Figure 3-4 shows the annual Waimakariri River sand loads for the period 1967 through 2017. Averaging 0.75 million m³, these range between 0.11 million m³ (2005) and 2.45 million m³ (1994). No statistically significant time trend was detected, although there appears to be a quasi-12-15-year inter-annual cycle in the 5-year running mean.

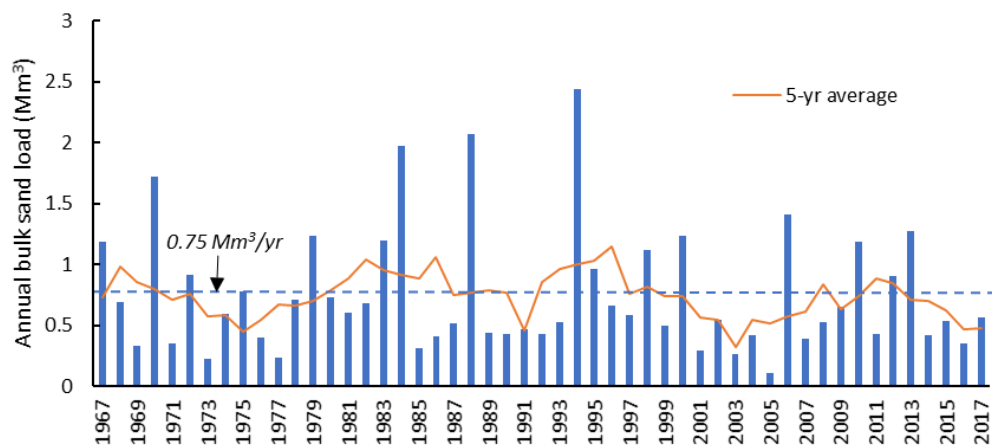


Figure 3-4: Annual bulk volume sand loads of the Waimakariri River. Orange curve shows a running 5-year average load; blue-dashed line shows the average annual load.

3.1.2 Sand removed with gravel extraction

Gravel is extracted from the bed of the lower Waimakariri River to prevent bed aggradation, which would otherwise increase flood risk, and to supply gravel and sand for roading and construction. While the Waimakariri River does not have the competence to transport its gravel bedload to the

coast along its low gradient tidal reach, the question has been raised as to whether sand extracted with the gravel would otherwise be delivered to the coast.

Gravel extraction volumes

Substantial gravel extraction has been taking place from the lower Waimakariri River channel for at least the last 60 years. ECan manage gravel extraction by monitoring river bed levels against a design ‘grade line’, set to maintain channel flood capacity and minimise any impacts associated with over extraction. Most of the extraction occurs in the reach between 18 and 4 km upstream from the coast, where the river’s gradient starts to reduce, diminishing the river’s capacity to transport gravel and prompting deposition (Figure 3-5). A gravel/sand transition occurs in the tidally influenced zone approximately 4 km from the coast, and from there downstream the Waimakariri River is a single-thread sand-bed river and carries no gravel bedload.

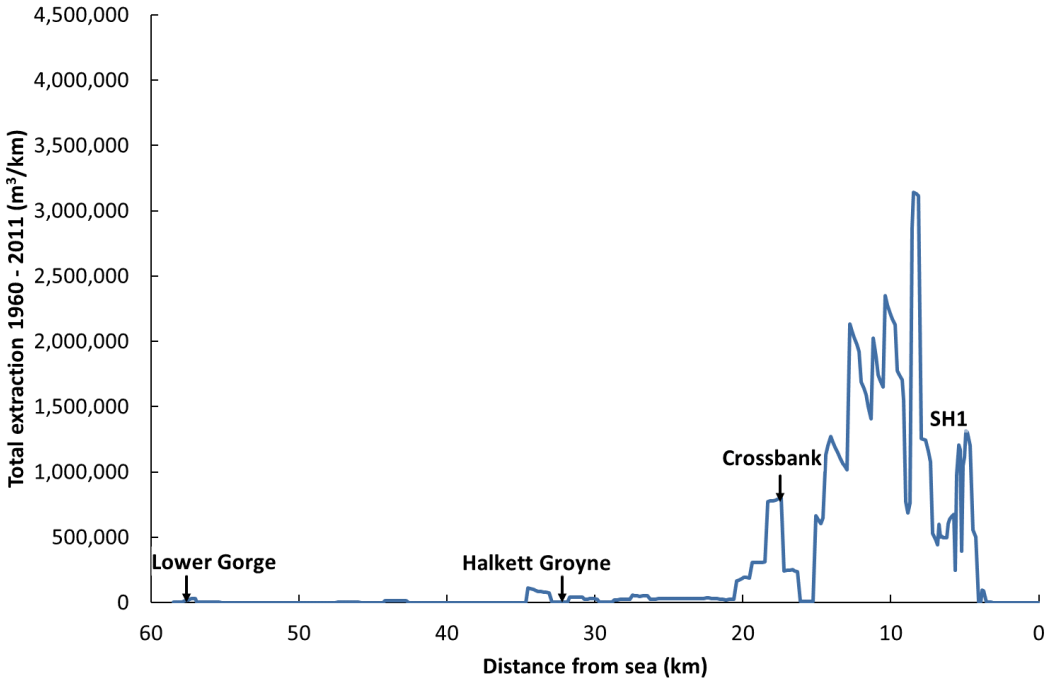


Figure 3-5: Location of gravel extraction along lower Waimakariri River. From Measures (2012).

Annual volumes of extraction from 1990 to 2017 are shown in Figure 3-6. The annual average extraction rate over this period was 344,000 m³/yr, with extraction over the last five years averaging 440,000 m³/yr.

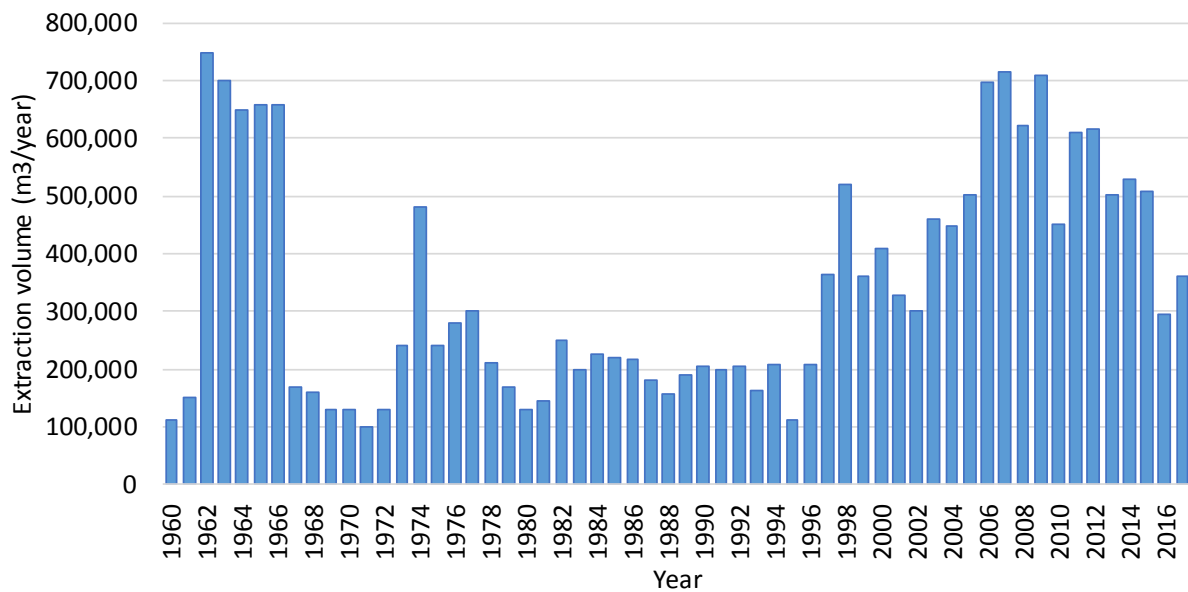


Figure 3-6: Annual Waimakariri River gravel/sand extraction since 1960. Data from Measures (2012) and ECan.

Bed material size-gradings

Material extracted from the gravel bed reach is a mixture of grain sizes, including gravels and sands. Bed material grain size data for the extraction reach is available from sampling conducted in 1959 by the North Canterbury Catchment Board (Stephen and Nottage 1959), and more recent data on size gradings from extraction stock piles was provided by extractors (Isaacs and Fulton Hogan). These data show (Figure 3-7) approximately 11% of the extracted material is in the sand range 0.063 to 0.5 mm that forms the bed material in the tidal reach (as sampled in this study, Table 3-1). This equates to an annual average extraction rate of 38,000 m³/yr of sand in this size range. This is equivalent to 4.9% of the estimated 746,000 m³/yr total sand delivery to the coast from the river (see above).

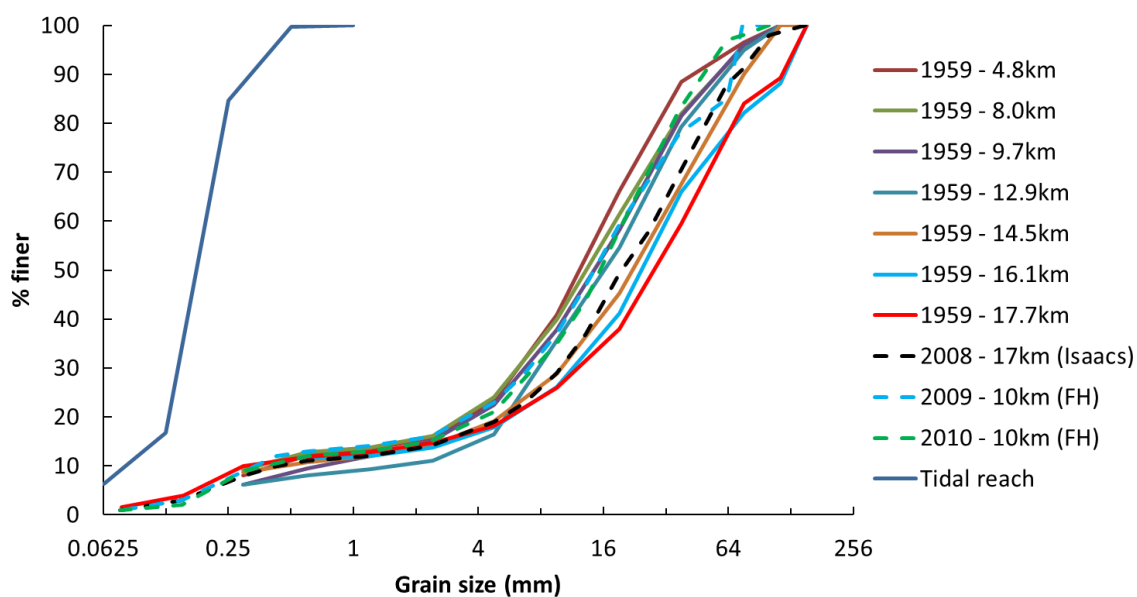


Figure 3-7: Waimakariri River bed-material size grading. Grain size data collated from 1959 catchment board sampling (Stephen and Nottage 1959), sampling by extractors (Isaacs and Fulton Hogan), and sampled from the tidal reach for this study. Note for the gravel samples the dominant gravel mode and the secondary sand mode matching that found in the tidal reach (which is largely finer than 0.5 mm).

However, when considering the effect of gravel extraction on coastal sand supply it is important to consider how the sand supply to the coast would change if extraction was ceased. If that happened, the currently-extracted sand would be buried within gravel deposits along the depositional reach, and so would be unavailable for transport further downstream. Bedload transport modelling conducted in 2012 investigated the effect of historic extraction by simulating the period 1967-2011 with and without extraction (Measures 2012). The modelling showed that whilst bed levels would be over 2.5 m higher in some parts of the depositional reach, there was very little effect on the position of the gravel/sand transition or bedload delivery to the tidal reach.

Thus, gravel extraction under the present regime of maintaining a design river bed-level profile, whilst intercepting the equivalent of 4.9% of the sand delivery to the coast, does not significantly affect the Waimakariri River's delivery of sand to the coast. Even if extraction stopped, most of the extracted sand would not reach the coast as it would remain locked up in river-bed gravel deposits.

3.1.3 Sand removed by irrigation water abstraction

Sand management practices

Water is extracted from the Waimakariri River for several purposes including irrigation, stock-water, and domestic supply. At the same time as removing water, suspended sediment is also removed. Sediment management practices at the different intakes vary (Table 3-2). Most of the largest takes have settlement ponds designed to collect suspended sand, but none of the ponds have sediment flushing capabilities, instead relying on mechanical excavation. At only one intake (Central Plains Water Ltd intake at Sheffield) is sediment returned to the river.

Table 3-2: Sediment management practices at the main surface water takes from the Waimakariri River and tributaries. Takes are listed from upstream to downstream.

Location/name	Consent holder(s)	Sediment management
Kowai River	Selwyn District Council	No settlement pond. Takes ceased (or blocked) during floods and freshes.
Sheffield	Central Plains Water Ltd	Effective settlement pond, all sediment returned to river bed.
Gorge Bridge	Selwyn District Council	No settlement pond. Intake proactively closed prior to freshes to prevent gravel entering intake tunnel.
Browns Rock	Waimakariri Irrigation Ltd Ngai Tahu Waimakariri District Council Glen Eyre Dairy Ltd	Settlement pond but sediment is not returned to river. Takes cease at 300 m ³ /s river flow.
Paparua scheme (Intake Road)	Selwyn District Council	Settlement pond. Ponds emptied mechanically but no sediment returned to river. Takes ceased (or blocked) during floods and freshes. Channel upstream of intake designed to try and minimise coarse sediment entering scheme.
Claxby scheme (Downs Road)	Claxby Irrigation Ltd	No formal settlement pond but settlement occurs in intake canal upstream of fish screen. Settled sediment excavated periodically but not returned to river. Small proportion of sediment returns to river via fish bypass.

Net sand removal

To calculate the amount of suspended sand removed from the river via water extraction, we first estimated the mean water extraction rate at each intake as a function of Waimakariri River flow. This considered the maximum take rate, minimum flow restrictions (as per the relevant consents), river flood shut-down thresholds (estimated after discussions with scheme operators), and seasonality of water demand (i.e., irrigation vs other uses). These parameters are listed in Table 3-3.

We then calculated the net suspended sediment extraction rate from the river based on the water extraction rate, the concurrent river discharge, the river's suspended sediment rating curve (as described in Section 2.1.1), the sediment return percentage (i.e., the proportion of suspended sediment returned to the river from the settling pond), and the river's flow duration curve. Assumptions regarding the calculation of sediment extraction rate at each take are summarised in Table 3-3. This also assumed an even distribution of flows throughout the year. In reality, flows are seasonally varying but given the small magnitude of the total extraction the effect of this assumption is acceptable.

Table 3-3: Parameters influencing estimated annual sediment take at each major surface water take from the Waimakariri River.

Take	Consent No (for details of low flow restrictions)	Maximum take (m ³ /s)	Flood cut-off (Waimakariri flow m ³ /s) ¹	Sediment return % ²	Seasonality (proportion of year)
Kowai	CRC155937	0.63	300	0%	100%
Sheffield	CRC136234 CRC175118	2.00 ³	900	90%	100%
Gorge Bridge	CRC155937	0.80	300	0%	100%
Browns Rock (stock-water)	CRC133965	2.10	300	0%	100%
Browns Rock (irrigation)	CRC166677 CRC172924 CRC176521	14.45	300	0%	50%
Paparua (stock-water)	CRC012006	1.33	500	0%	100%
Paparua (irrigation)	CRC012006	0.80	500	0%	50%
Claxby	CRC152927	1.93 ⁴	900	5%	50%

¹ Flood cut off thresholds were estimated after discussion with scheme operators. In practice thresholds are often flexible and depend on river conditions (e.g., debris or gravel build-up).

² Sediment return percentage estimated based on sediment management practices described in Table 3-2.

³ Central Plains Water Limited (CPWL) consents allow extraction of up to 25 m³/s but due to changes in scheme design only a maximum of 2 m³/s is utilised. There are no plans to make use of the rest of this consented amount (Fiona Crombie, CPWL, pers. comm.).

⁴ Claxby Irrigation Ltd consents allow extraction up to 1.610 m³/s. However, additional water is taken into the upstream 1.6 km of headrace canal then returned to the river via the fish screen bypass (pers. comm. Paul Reese). This additional volume is not monitored and we have assumed it to be 20% of the consented flow.

The overall mass of suspended sediment removed from the Waimakariri River via water extraction was estimated to be 61,000 t/yr, equivalent to 2.0% of the river's measured suspended load. Assuming that the irrigation takes only collect from the measured suspended load (and do not extract bedload), and allowing (from above) that the sand content of the measured suspended load is 21.6%, then the net sand extraction rate associated with water extraction is 13,200 t/yr (equating to 8,300 m³/yr assuming a bulk density of 1.6 t/m³). This amounts to 1.1% of the river's sand discharge to the coast.

This estimate should be considered as an upper bound for two reasons:

- Scheme operators try to minimise the amount of sediment entering the intake while undertaking physical works in the river to maintain river flow at the intake. For example, at the Paparua intake of Selwyn District Council (SDC) the approach channel leading to the intake gate is maintained in such a way as to preferentially direct low sediment concentration water towards the gate and to bypass high sediment concentration water (Daniel Meehan, SDC, pers. comm.).
- Irrigation water users do not extract their full consented volume throughout the irrigation season. Water use is often less: for example, when there has been rain on the Canterbury Plains and irrigation demand is low. This has been partially accounted

for in our assessment by assuming a 6-month irrigation season, when in reality some irrigation often occurs outside this window.

3.1.4 Entrapment downstream of SH1, particularly in Brooklands Lagoon

Brookland Lagoon

Hicks and Duncan (1993) analysed repeat cross-section surveys of Brookland's Lagoon between 1932 and 1969, a period which captured the northward shift of the Waimakariri River mouth to its present location at Kairaki. They estimated an average entrapment rate of 38,000 m³/yr (bulk volume) of silt and sand over this 37-year period, but noted an exponential decline in this rate and considered that the current sedimentation rate (i.e., in 1993) was likely around a few mm/yr, equating to about 4,000 m³/yr of entrapment. Figure 3-8 shows their plot of volumetric change since 1932. They noted that some of the sediment accumulation since 1940 resulted from storm-wave wash-over from the open-coast beach, while the spit was initially low, and from wind-blown sand from the beach.

A subsequent cross-section survey was apparently completed in 2007/8 (as mentioned by Cooper as reported in Boyle 2011). However, we have found no analysis from this on sedimentation rates apart from a mention that this survey showed recent sedimentation rates of up to 3 mm/yr at the southern (Spencerville) end of the lagoon but no net sedimentation at the northern end. Estimating a lagoon area of 170 hectares and a spatially averaged sedimentation rate of 1.5 mm/yr suggest a sediment entrapment rate of 2550 m³/yr, which is similar to Hicks and Duncan's estimate from 1993. Bolton-Ritchie (2007) observed that the lagoon bed sediment gets progressively muddier towards Spencerville while between 1977 and 2005 the proportion of sand in the lagoon bed sediment had decreased.

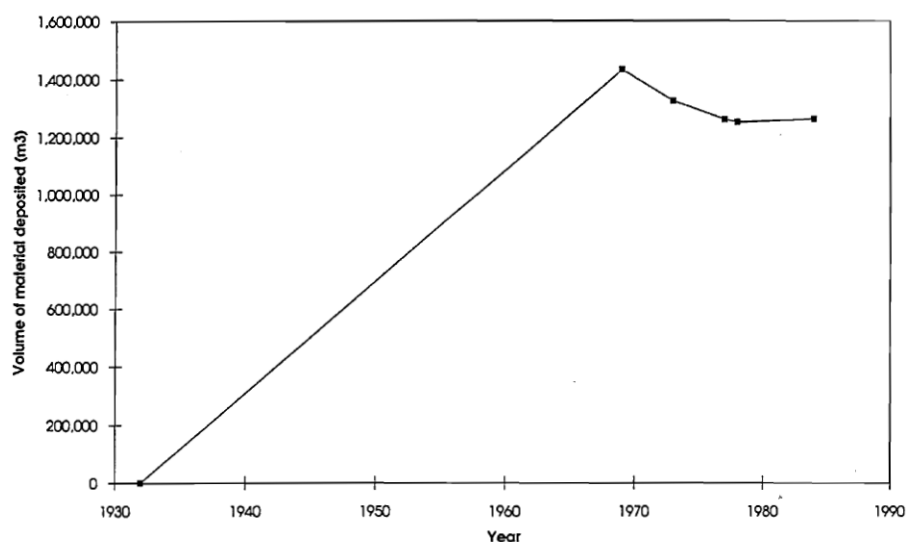


Figure 3-8: Brooklands Lagoon volume changes between 1932 and 1984. From Hicks and Duncan (1993). Volumes were determined from surveyed cross-section changes.

Most recently, Christchurch City Council (2010, page 54) reported some ongoing sedimentation:

There is evidence that Brooklands Lagoon/Te Riu o Te Aika Kawa is continuing to fill appreciably. Sediment laden water certainly does fill the estuary during flooding of the Waimakariri River and this drapes a

covering of mud a few millimetres thick over the bed of the estuary. This sediment is, however, easily resuspended by wave action and much may be removed from the estuary with outgoing tides. The chances of injection of coastal sand into the estuary from wind-blows and/or storm wash-over should lessen progressively as Brooklands Spit/Kairaki grows in width and height and is stabilised by vegetation, especially pine trees. The likelihood of another major migration of the Waimakariri River mouth should also diminish for the same reasons.

In summary, the general conclusion from the literature is that while Brooklands Lagoon continues to trap Waimakariri River sediment, this is now mainly mud grade, with deposition focussed towards the southern end of the lagoon. There appears to be little net exchange of sandy bed material between the river and the northern end of the lagoon. Moreover, little river-sourced sand appears to be recycled into the lagoon by wind-blow from the open coast, by virtue of the high, vegetated dunes on the Brooklands Spit. Thus, an upper limit estimate of current sand entrapment in Brooklands Lagoon from the Waimakariri River's suspended load (carrying 21.6% sand) is $2550 \times 0.216 = 550 \text{ m}^3/\text{yr}$.

Tidal reach of Waimakariri River

We have assumed that the Waimakariri River channel between SH1 Bridge and the contemporary mouth at Kairaki is neither trapping sand nor eroding but is in a state of dynamic equilibrium on a long-term average basis, thus it has no impact on the coastal sediment budget. This assumption is based on a lack of issues relating to ongoing sediment accumulation or scour. While there have been localised transient channel engineering issues relating to bank erosion and bar growth (Tony Boyle, ECan, pers. comm.), there would appear to be no trends for increasing or decreasing channel volume. Similarly, erosion and sand bar growth at the spit tip on the south side of the river mouth appear to be short term processes (Boyle 2011).

3.1.5 Synthesis of coastal sand discharge from the Waimakariri River

Summarising the results from the sections above:

- The estimated mean annual Waimakariri River (bulk volumetric) sand discharge into its tidal reach is $746,000 \text{ m}^3/\text{yr}$. The standard error on this is $\pm 6.5\%$ ($\pm 48,000 \text{ m}^3/\text{yr}$).
- Gravel extraction operations from the lower Waimakariri River channel remove about $38,000 \text{ m}^3/\text{yr}$ of sand, but this should not impact the coastal sand discharge since if the extraction did not occur this sand would be deposited in the aggrading riverbed.
- Sand is removed permanently from the Waimakariri River via irrigation water takes at a rate of up to $8,300 \text{ m}^3/\text{yr}$ (but almost certainly at a lesser rate). This is well inside the uncertainty of the sand discharge estimated above. Note also that:
 - this figure would certainly reduce if all water takes returned sand trapped in settling ponds to the river, which is typically not the case at present, and
 - the irrigation takes are all upstream from SH1 Bridge, so their effects are already captured in the sand load estimated there.
- Brooklands Lagoon and the tidal reach of the Waimakariri River intercept less than $1,000 \text{ m}^3/\text{yr}$ of sand.

- Thus, the contemporary net Waimakariri River sand discharge to the coast is 745,000 m³/yr. Without irrigation this would increase marginally up to 753,000 m³/yr.

3.1.6 Proportion of river sand load retained on shore

As detailed in Section 2.1.5, the proportion of the Waimakariri River sand load retained on the beaches of southern Pegasus Bay was assessed by aligning the size grading of the river load with representative beach sediment size gradings. This provided trap efficiencies for each size fraction.

The results are shown in Figure 3-9 and summarised in Table 3-4. The results using the foreshore size gradings from Blake (1967) and ECan (1997) are very similar, with quite low trap efficiencies for very-fine sand (7% and 4%, respectively) and an overall sand trap efficiency on the foreshore of 37% and 35%. These results should be representative of the upper beach profile, but they likely underestimate the trap efficiency for the submerged lower profile, hence they provide a minimum estimate of the overall trap efficiency for the full profile.

The Allan et al. (1999) data suggest significantly higher trap efficiencies for the fine and very-fine sand fractions and over all sand fractions (56%-58%); moreover, the trap efficiencies for fine and very-fine sand increase as the averaging distance is increased seaward, as is expected. However, the dissimilarity between the Allan et al. results averaged across the foreshore to the MSL contour and those averaged over the same span of profile from the ECan data raise a question around the representativeness of the Bridge Street data. Also, the small difference observed between averaging to MSL and averaging to 7.5 m and 11 m depths with the Allan et al. data suggest that foreshore results may be reasonably indicative of the overall beach profile.

On that basis, we have assumed that the average foreshore sand trap-efficiency indicated from the Blake and ECan data (36%) may be applied to the overall beach profile, albeit with the expectation that the true trap efficiency will be a little higher. In other words, we assume that a minimum of 36% of the Waimakariri River's sand will be retained on the beach profile above closure depth.

Table 3-4: Trap efficiency factors by size fraction for river sediment retention on beaches. Determined by aligning river sand load and beach sand size distributions. Data from Allan et al. (1999) is from Bridge Street and is averaged across the beach profile from the foreshore to the given location. Blake (1967) data is averaged along southern Pegasus Bay from mid-foreshore samples. ECan data is averaged along southern Pegasus Bay from foredune, upper-foreshore, and mid-tide samples.

	Blake (1967)	ECan (1997)	Allan et al. (1999) – Bridge St		
	Mid Foreshore	Foreshore average	To MSL contour	To 7.5 m depth contour	To 11 m depth contour
Coarse sand	1	1	1	1	1
Medium sand	1	1	1	1	1
Fine sand	0.55	0.525	0.79	0.7	0.66
Very-fine sand	0.07	0.04	0.23	0.35	0.41
Mud	0	0	0	0	0
All sand	0.37	0.35	0.56	0.57	0.58

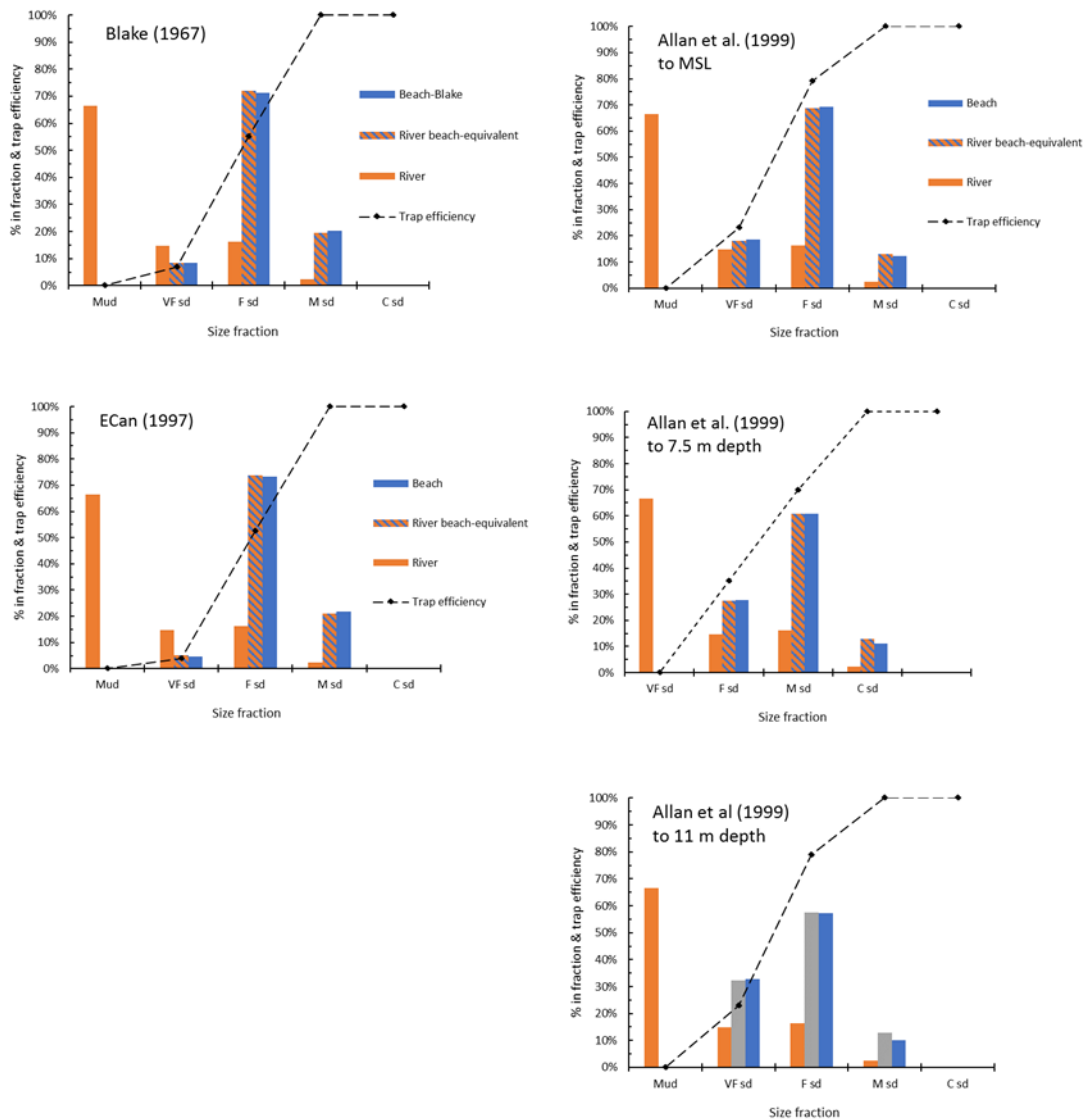


Figure 3-9: Size distributions of river suspended load, beach sand, and beach-trapping efficiency by size fraction. Trap efficiencies were adjusted until river beach-equivalent distributions and beach sand size distributions aligned. Data from Allan et al. (1999) is from Bridge Street and is averaged across the beach profile from the foreshore to the given location. Blake (1967) data is averaged along southern Pegasus Bay from mid-foreshore samples. ECan data is averaged along southern Pegasus Bay from foredune, upper-foreshore, and mid-tide samples.

3.2 Longshore transport rates

3.2.1 Wave-driven longshore transport patterns

Figure 3-10 shows the alongshore patterns of mean annual northward, southward, net, and gross longshore transport along the Pegasus Bay, as determined from the SWAN modelling for the period 1 September 2000 through 31 December 2017 and using Equation (5) with the efficiency factor (K) set equal to 0.21 (the basis of this K value is explained in Section 3.2.3).

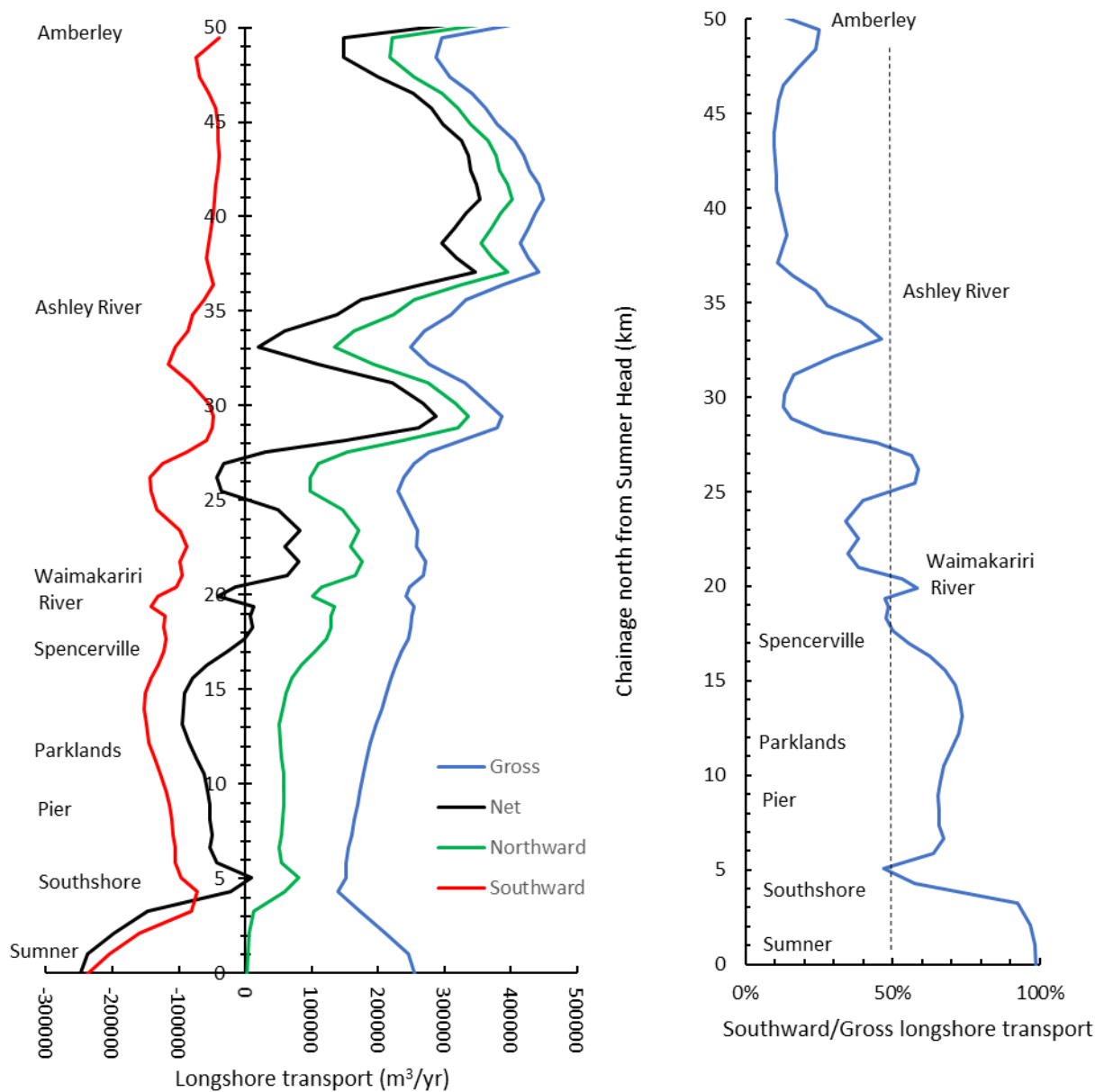


Figure 3-10: Alongshore distribution of mean annual northward, southward, net, and gross longshore sand transport, as predicted from SWAN wave modelling. Plot on right shows ratio of southward to gross longshore transport.

Note:

- A general trend for intensifying northward transport going north along the Pegasus Bay shore, consistent with reducing shelter from southerly swells further north from banks Peninsula.
- An opposite trend for generally intensifying southward transport towards the southern end of Pegasus Bay.
- A reversal of the net drift direction: southwards south of the Waimakariri River; northwards north of the Waimakariri River.

- A reasonably uniform gross transport along the bay, apart from close to Banks Peninsula.
- Significant local fluctuations in the longshore transport (e.g., compare at 27 km and 30 km chainage), which we infer mostly relate to wave refraction effects across relief in the Pegasus Bay bathymetry, notably the Pegasus Canyon and the Banner Bank (Figure 3-11).
- We suggest the results are unreliable for the southern-most 3 km of the shore because of the failure of the assumption of shore-parallel bathymetry contours used when shoaling the waves to the breakpoint, due to the topography of the Avon-Heathcote ebb-tidal delta and Sumner Head.

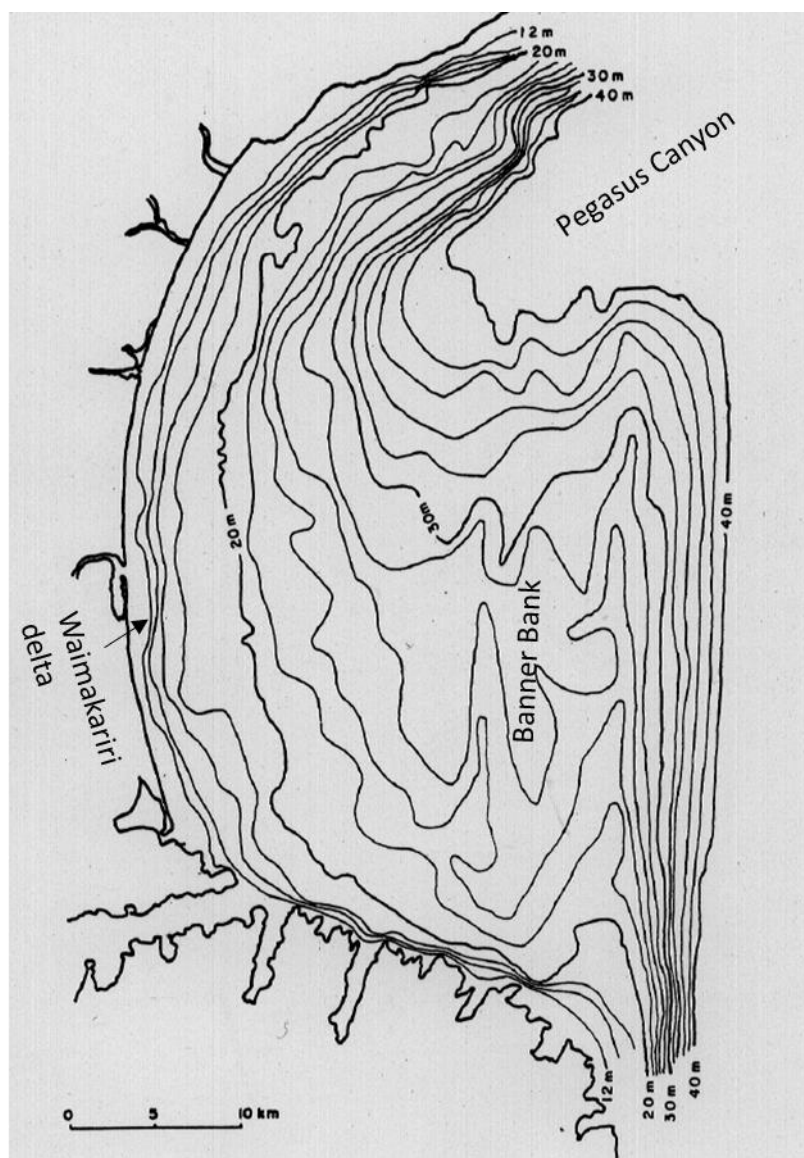


Figure 3-11: Pegasus Bay bathymetry. From Campbell (1974).

These findings are consistent with the general qualitative appreciation of longshore transport patterns along Pegasus Bay (e.g., as summarised in Allan et al. 1999), and so vindicate the use of the full spectral wave refraction approach in the SWAN model for this study (rather than using

parameterised waves as done by Gorman et al. 2002, who found apparent net northward transport all along Pegasus Bay).

Of particular interest to this study is the general trend for intensifying southward net transport between the Waimakariri River mouth and Bottle Lake (chainage 21 km to 14.8 km), then a quasi-steadily decreasing transport rate towards Southshore (chainage 5 km). An alongshore-increasing net transport rate in the direction of transport (i.e., positive transport divergence) suggests an eroding shore, while an alongshore-decreasing rate indicates deposition (Figure 3-12).

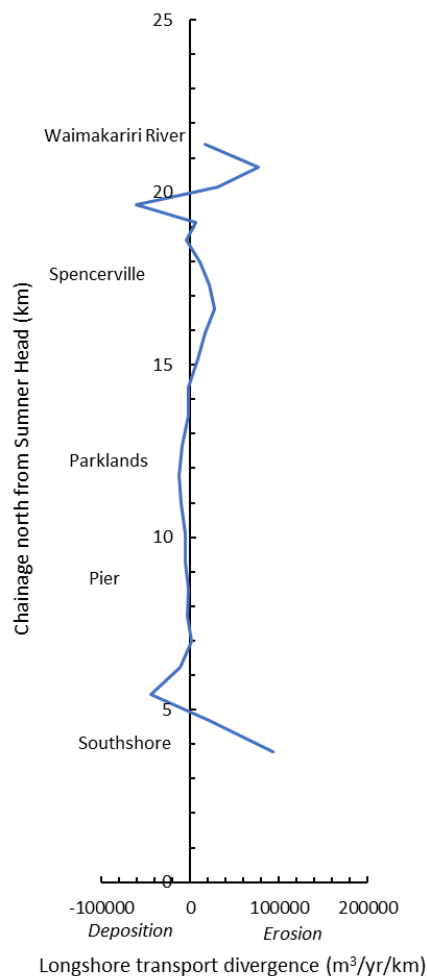


Figure 3-12: Long-term average net longshore transport divergence. Positive transport divergence signals erosion; negative divergence signals accretion.

Transport-divergence-driven deposition between chainage 14.8 km and 5 km is consistent with the surveyed progradation along this shore (see Section 3.3.1), but divergence-driven erosion closer to the river mouth is not consistent with the surveyed accretion of this span of shore. We interpret that this apparent discrepancy arises because river sand deposited outside the surf-zone by the outflow jet of the Waimakariri River during floods is also transported southwards from the river mouth outside of the surf-zone by other processes (most likely the momentum of the river flood discharges but likely also influenced by tidal and shelf currents) before the river sand is eventually washed onshore by waves. Thus, along this span of shore, the gradually intensifying southward surf-zone transport is “fed” by onshore transport of river sand, which arrives onshore in quantities sufficient to

result in shore accretion. This interpretation is consistent with bathymetry charts that show an elongated offshore delta skewed south some 5-6 km from the Waimakariri River mouth (Figure 3-11).

3.2.2 Temporal variation in net longshore transport rate

A time-series of the longshore transport potential based on the SWAN modelling is shown in Figure 3-13 for chainage 12.1 km at Waimairi Beach. We expect this site to be reasonably representative for temporal patterns. The largest daily transport rates occur in association with north-easterly quarter waves; the largest occurring on 26 May 2011. Apart from around this event, the trend of the cumulative transport plot is quasi-linear, indicating a generally-steady net transport rate with little inter-annual variability. On this basis, we consider it reasonable to assume that the annual average longshore transport potential over the period 2000-2017 should also represent the somewhat longer period (1990-2017) covered by the beach profile dataset.

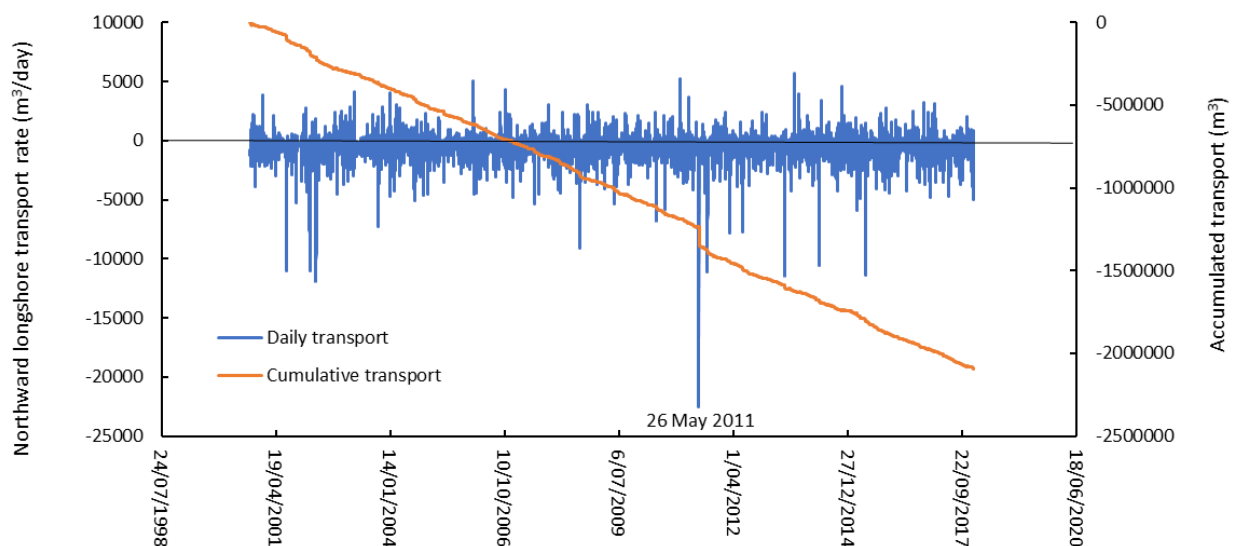


Figure 3-13: Daily longshore transport rates and time-cumulative longshore transport at Waimairi Beach (chainage 12.1 km).

3.2.3 K-factor calibration

Following on from the above discussion, we calibrated the efficiency factor, K , in the CERC longshore transport formula (Equation 1) by matching the net southward longshore transport at chainage 14.8 km (at the northern end of the shore-span with negative transport divergence and associated accretion) with the longshore-accumulated rate of sand accretion over the upper and lower beach profile to the south of that point. In other words, we calibrated the transport model so that all the accretion detected across the beach profile to the south of this point could be supplied by surf-zone longshore transport from the north.

3.2.4 Proportion of Waimakariri River sand transported south

The longshore transport regime at the Waimakariri River mouth is bi-directional. We estimated the proportion of the river's sand moved south from the ratio of time-averaged southward transport to time-averaged gross transport (i.e., the sum of northward and southward transport) at the river mouth. Since that ratio varied within several km of the river mouth (Figure 3-10), we extracted a

spatially-averaged value of 68% – that is, 68% of the river sand should be transported south. This value should be regarded with some uncertainty, however, since, as discussed above, the processes moving sand away from the river mouth extend beyond wave-driven surf-zone transport. The only way to refine this estimate, however, would be with a calibrated, quasi 3D, hydrodynamic morphological model that simulated sediment transport by the river outflow along with waves and other current drivers (e.g., the XBeach model). This was beyond the scope of the present study.

3.2.5 Importance of other current drivers – Sensitivity analysis

The uncalibrated XBeach runs with the simplified shore model explored the sensitivity of the wave-driven longshore transport to the effect of nearshore winds and currents acting in the opposite direction to the wave-driven longshore current. Figure 3-14 shows the cross-shore distribution of longshore transport for the five scenarios tested (only waves, waves + typical wind, waves + strong wind, waves + weak current, waves + strong current), while Table 3-5 compares the peak local transport and the longshore transport integrated across the beach profile (note that because the model XBeach model was uncalibrated, attention should be given to the relative differences in these results rather than the absolute values).

The scenario with a typical NE wind blowing against the wave-driven longshore current (Scenario 2) only reduces the peak and cross-shore integrated transport by a few % - effectively, the wind stress over the surf-zone slows the wave-driven longshore current by a small amount. With a stronger wind (Scenario 3), the northward wave-driven current and sand transport remain dominant in the surf-zone, but minor reverse (southward) transport occurs outside the surf-zone, reducing the net northward transport integrated over the whole profile. Under different scenarios with the wind assisting the wave-driven surf-zone longshore current, we would expect transport enhancements of similar proportions. From this we conclude relatively minor overall effects of neglecting local wind stress on the time-averaged transport determined by a waves-only longshore transport formulation.

The scenario with a weak (0.2 m/s) south-setting externally forced current (Scenario 4) reduces the peak and cross-shore integrated transport somewhat more than does the typical wind case (22% reduction in cross-shore integrated transport) by reducing the northward transport in the surf-zone and by driving some reverse (southerly) transport outside the surf-zone. The stronger current intensifies this effect and results in a net southward transport over the whole profile, even while the transport within the surf-zone remains northward. However, while currents larger than 0.2 m/s have been observed and predicted in Pegasus Bay, they appear to be largely tidally-forced and are therefore unlikely to be sustained for more than a few of hours and reverse twice daily – thus their residual impact on net longshore transport should be less than indicated in Table 3-5. Again, under different scenarios with tidal and/or oceanic currents assisting the wave-driven surf-zone longshore current, we would expect transport enhancements of similar proportions, so the net effect averaged over time should cancel to some degree. Nonetheless, we conclude that externally-forced currents could have a measurable effect on the time-averaged transport determined by a waves-only longshore transport formulation.

We caution that the above results are from ‘conceptual’, uncalibrated XBeach simulations hence they should be interpreted only semi-qualitatively. The only way to properly evaluate this would be via a fully calibrated XBeach model set-up for the study shore, and this would require being coupled to the spectrally-refracted wave buoy record and a calibrated shelf-scale hydrodynamic model for which there are no boundary condition data available for the past 17 years to match the wave buoy record. A directional wave record collected for several years from 2007 at 3 km offshore from Jellicoe Street

(McConnell Dowell 2007) could provide either an alternative wave boundary condition or validation data.

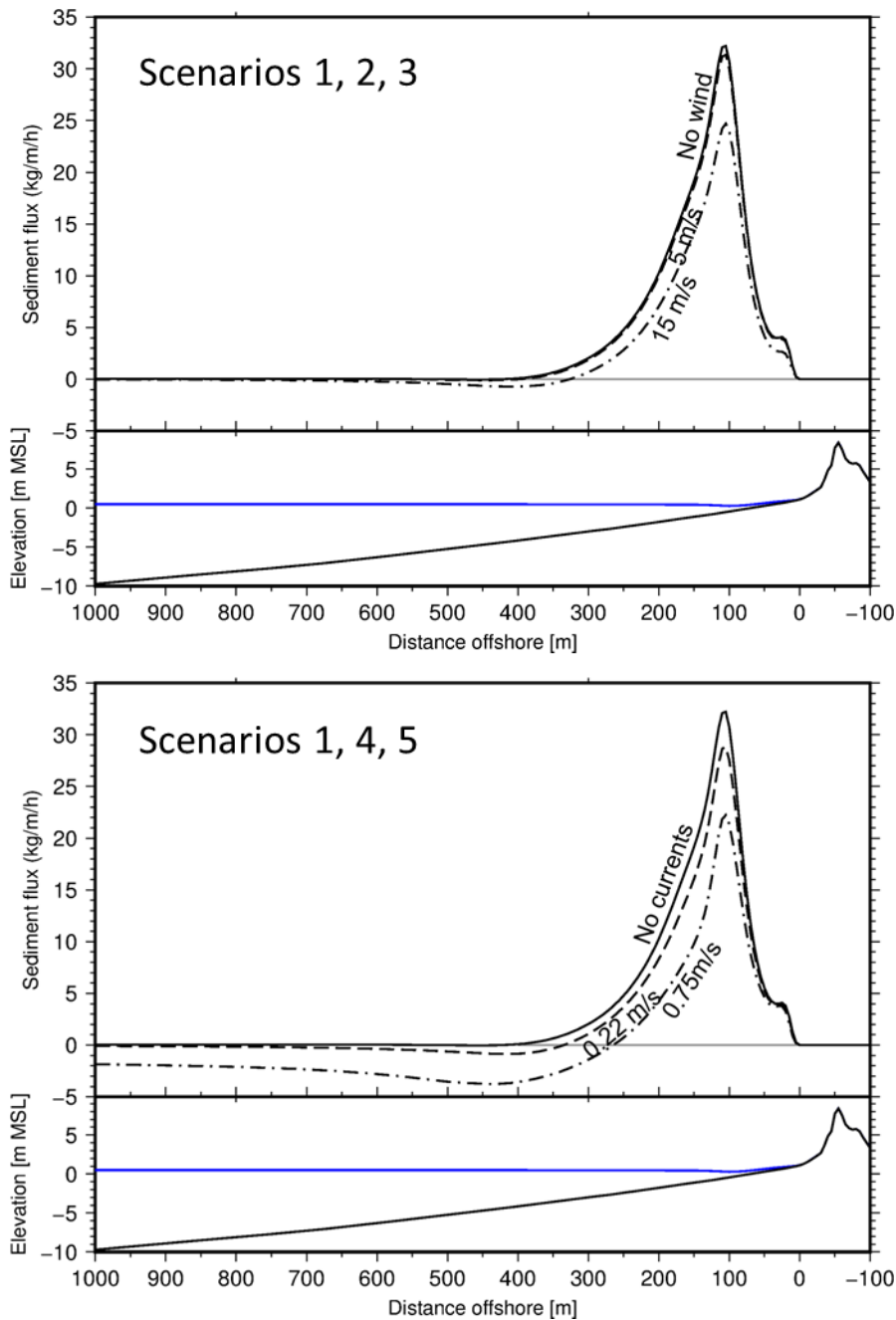


Figure 3-14: Cross-profile distribution of longshore transport simulated by XBeach model for different wave, wind, and externally-forced current scenarios. Top plot shows effects of waves + counteracting winds; lower plot shows effects of waves + counteracting externally-forced current. Positive transport is to the north; negative to the south.

Table 3-5: XBeach model results showing effect of counter-acting wind and current on wave-driven longshore transport. Figures in brackets show % transport relative to waves-only scenario. Peak transport is highest longshore transport rate across beach profile. Positive transport is to the north; negative to the south.

Scenario	Waves	Wind	Current	Peak longshore transport (kg/m/h)	Total net longshore transport over profile (t/h)
1	1 m from E	X	X	31.6	3.60
2	1 m from E	5 m/s from NE	X	30.9 (98%)	3.47 (96%)
3	1 m from E	15 m/s from NE	X	25.3 (80%)	2.45 (68%)
4	1 m from E	X	0.22 m/s to SE	28.8 (91%)	2.79 (78%)
5	1 m from E	X	0.75 m/s to SE	22.2 (70%)	-1.10 (-31%)

3.3 Sand volume changes on Christchurch City beaches

Our assessment of sand retention on the project beaches included:

- Analysing sand volume changes in the foreshore-backshore out to and above the MSL contour from ECan’s profile survey dataset.
- Estimating the depth of the effective seaward limit, or closure depth, of the nearshore segment of the beach profile, and assuming that sand volume changes on this lower beach would occur in proportion to those on the upper beach.

3.3.1 Upper beach volume analysis

Our analysis of the ECan beach profile dataset for the study shore produced records of unit sand volume (m³/m) on each profile above the MSL datum, split between the backshore (landward of the foredune toe) and the foreshore (seaward of the foredune toe), from 1990 through to 2017.

Space-time patterns

An overall space-time view (i.e., alongshore and over time) of volume changes is provided by the ‘dispersion’ plot of combined backshore and foreshore changes (Figure A). This shows:

- A general trend for increasing beach volume over time (indicated by the general progression from blue to brown shading from the bottom to top of the dispersion plot).
- Synchronous volume changes along most of the shore (horizontally-elongated polygons), assumed to be associated with cross-shore sand cycling between the foreshore and nearshore bars during storms and recovery periods (as indicated by aligning blue polygons with events of high onshore wave energy flux, allowing for up to a 6-month time lag between the event and the next ECan survey).
- An exception is the shore adjacent to the Avon-Heathcote Inlet, where volume-change cycles indicate quasi five-ten yearly cycles of accretion and erosion associated with trimming and recovery of the Southshore spit and bars coming onshore from the ebb delta flanks.

- Another exception is at the Waimakariri River mouth, where the patterns are indicative of inter-annual changes at the tip of the Brooklands spit – for example, the erosion phase of the spit tip beginning about 2008 (as reported by Boyle 2011) shows clearly.
- A sand wave appears to have migrated southward from the Waimakariri River mouth, beginning from about 2000 and migrating about 0.5 km per year (as indicated by the pink ridge trending obliquely up the plot). Figure 3-4 shows that Waimakariri delivered its largest annual sand load (over three times its average sand load) in 1994, so this may be the source of the sand wave, allowing that it could take several years for the sand to move onshore off the river delta. Possibly also, the sand wave could have been initiated by a phase relatively higher southward longshore transport that increased the proportion of the river sand load that was transported south.
- A major phase of accretion commenced from early 2011 immediately adjacent to the Avon-Heathcote Inlet. We discuss how that may be associated with earthquake effects on the estuary in Section 3.4.

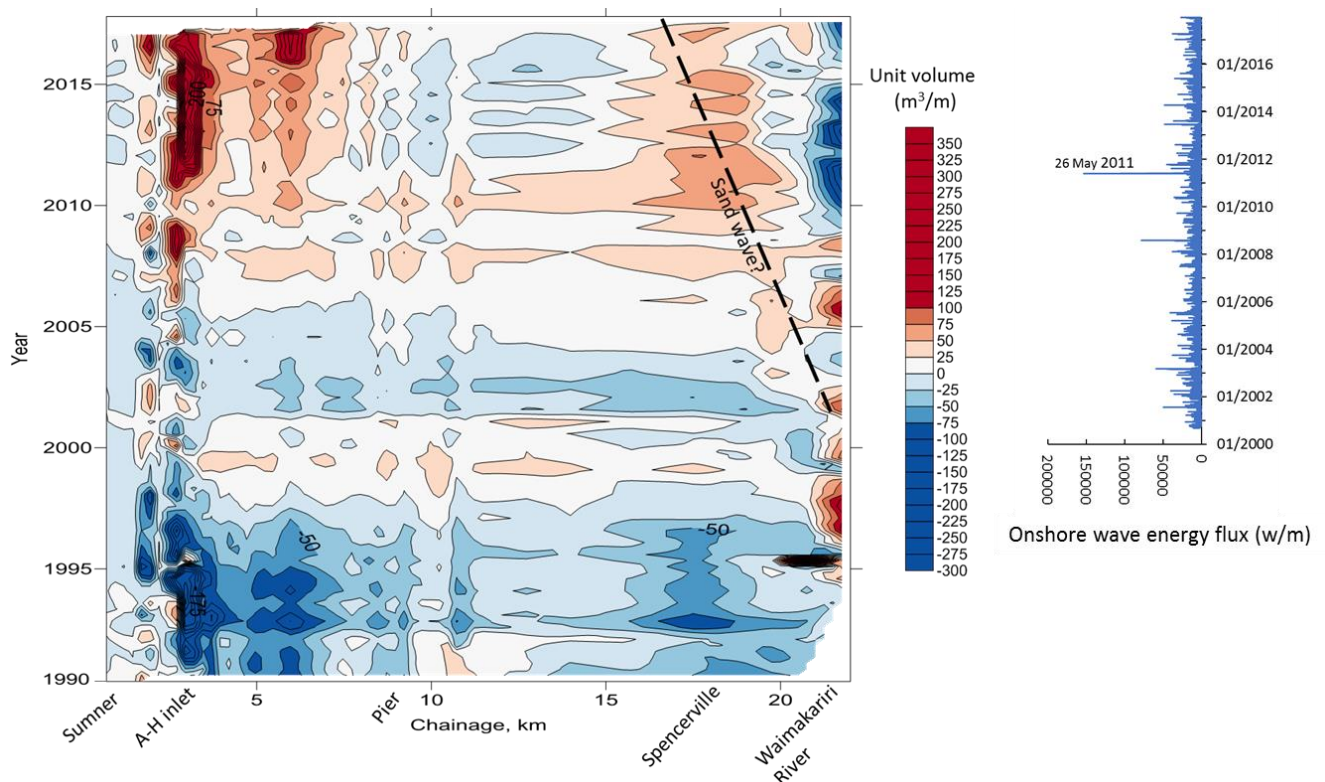


Figure 3-15: ‘Dispersion plot’ showing space-time patterns of unit volume for backshore and foreshore combined. Chainage indicates distance north alongshore from Sumner Head. Unit volumes at each profile are residuals from the temporal mean volume over all surveys. Dashed diagonal line suggests a migrating sand wave. Plot to right shows onshore wave energy flux near Pier, aligned in time with dispersion plot. Data record begins in May 1990.

Time trends in unit volume gain

Figure 3-16 shows the alongshore variation in the linear trend rate of unit volume change for the 1990-2017 period. This shows accretion focussed in two main areas: between the pier and the Avon-Heathcote Inlet, and the Bottle Lake – Brooklands Spit area (except for the northern tip of Brooklands Spit at the Waimakariri River mouth). The shore appears to be quasi-stable at Waimairi Beach and Parklands (10 km and 12 km chainage) and at Sumner Beach.

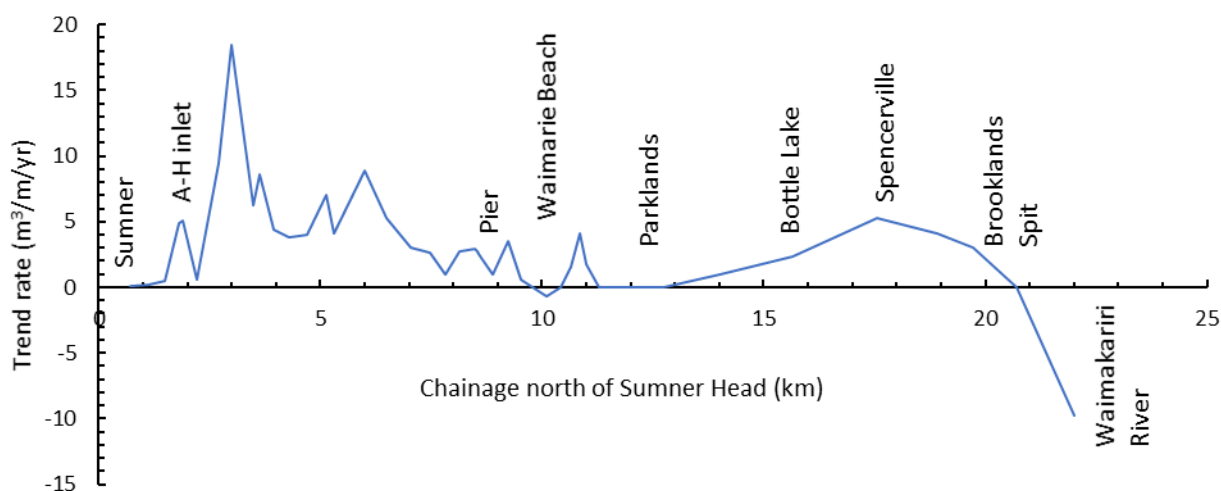


Figure 3-16: Trend rates for unit volume gain combined over backshore and foreshore at ECan profiles, 1990-2017.

Volume changes in littoral cells

The unit volume changes at each profile were accumulated into the 13 morphologically-similar littoral cells defined in Table 2-1 (including cells A-G defined by Tonkin and Taylor 2017). Beach volume accumulation rates for these cells between 1990 and 2017 are shown in Figure 3-17. The cells accumulating most sand are the northern Bottle Lake cell, Cell D (South New Brighton), and Cell G (Southshore spit). Most of the accumulation (80% overall) occurs in the backshore, as expected on an accreting shore. At the northern Bottle Lake cell, the foreshore has also lost sand overall. Taylors Mistake Beach has had minimal sand accumulation.

The 1990-2017 net volume accumulation rate totalled between Sumner Beach and the northern tip of Brooklands Spit is 56,700 m³/yr. This total increases to 63,000 m³/yr if we exclude the currently eroding profile at the Brooklands Spit tip beside the Waimakariri River.

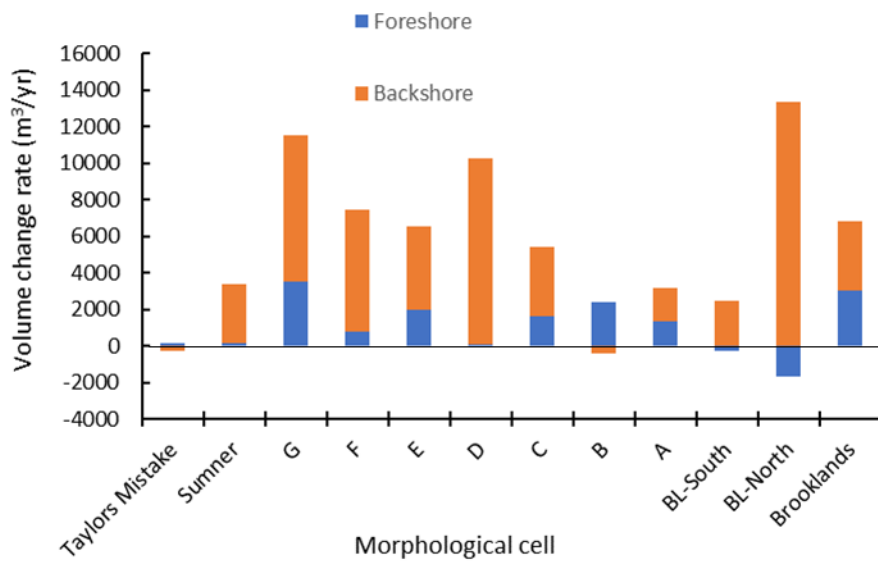


Figure 3-17: Average volumetric change rates in backshore and on foreshore within morphological cells. Where both backshore and foreshore rates are positive, the combined bar height indicates the net volume change rate.

3.3.2 Shoreline change rates

Linear trends were also fitted to the surveyed positions of the foredune toe and MSL ‘shorelines’ at the ECan profiles. As shown in Figure 3-18, the alongshore patterns were generally similar for both shorelines, indicating generally parallel seaward translation of the profile at rates that varied alongshore. The rates for the two shorelines diverged adjacent to the Avon-Heathcote inlet and along the Bottle Lake shore. The greater MSL accretion rate adjacent to the inlet can be related to a wider beach with sand bars associated with the inlet system. Along the Bottle Lake shore, the MSL line position has been quasi-stable while the dune toe has advanced, indicating a narrowing foreshore. The erosion trend at the northern tip of Brooklands Spit is dominated by the erosion phase that began there about 2008. We consider that this is driven by inter-annual river mouth cycles, likely associated with the shape and size of the river mouth bar.

In following sections, we assume that the average of the foredune toe and MSL shoreline trends should represent the overall trend for profile advance. Excluding the eroding site at the tip of Brooklands spit, the alongshore average of this profile advance trend is 0.51 m/yr. It varies from 2.7 m/yr at the Avon-Heathcote inlet to -0.25 m/yr (i.e., erosion) just north of the New Brighton pier.

As should be expected, the average shore advance trend aligns well with the combined foreshore and backshore upper beach volume trend (Figure 3-19).

We note that these time-averaged rates of shoreline shift mask considerable inter-annual variability. As observed in the previous section from Figure 3-15, the foreshore volume changes typically vary synchronously alongshore in quasi annual cycles relating to cross-shore sand exchanges associated with storm and recovery cycles. However, near the Waimakariri River mouth and the Avon-Heathcote inlet, the cycles span longer periods (of order 5-10 years) and have larger amplitude, and we infer that these relate to river mouth and inlet processes, including shoreward bar migration from the river and ebb-tidal deltas and spit-tip erosion and accretion cycles. Certainly, the shoreline of the

Southshore spit tip has been observed to be very “volatile” over the past century (John Walter, CCC, pers. comm.).

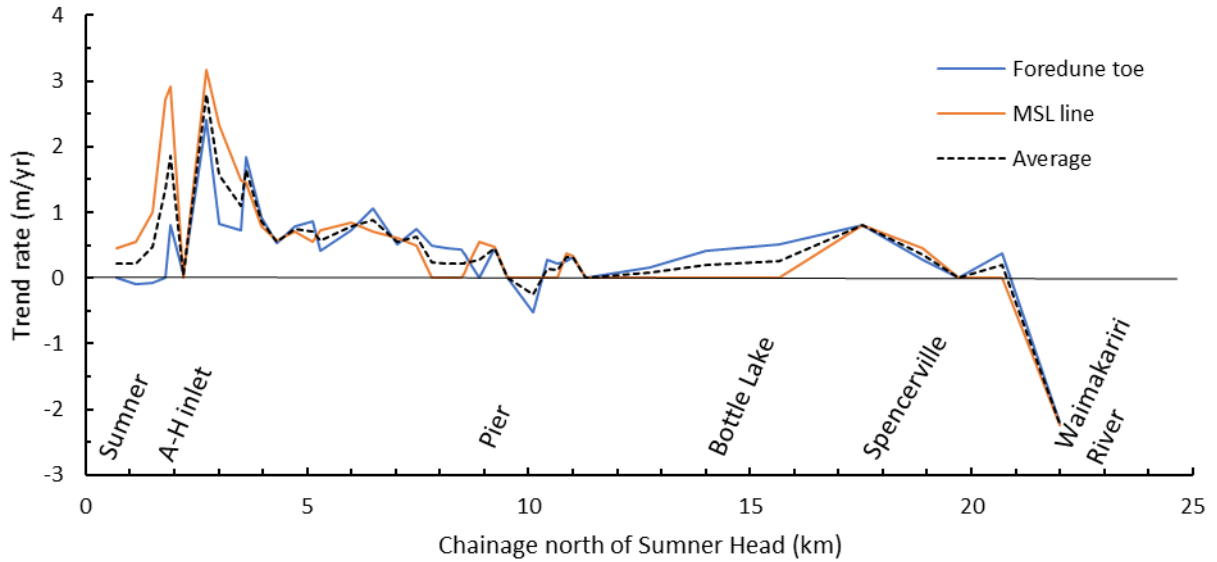


Figure 3-18: Trend rates for position of foredune toe and MSL line at ECan profiles, 1990-2017. Dashed line averages the foredune toe and MSL line trends.

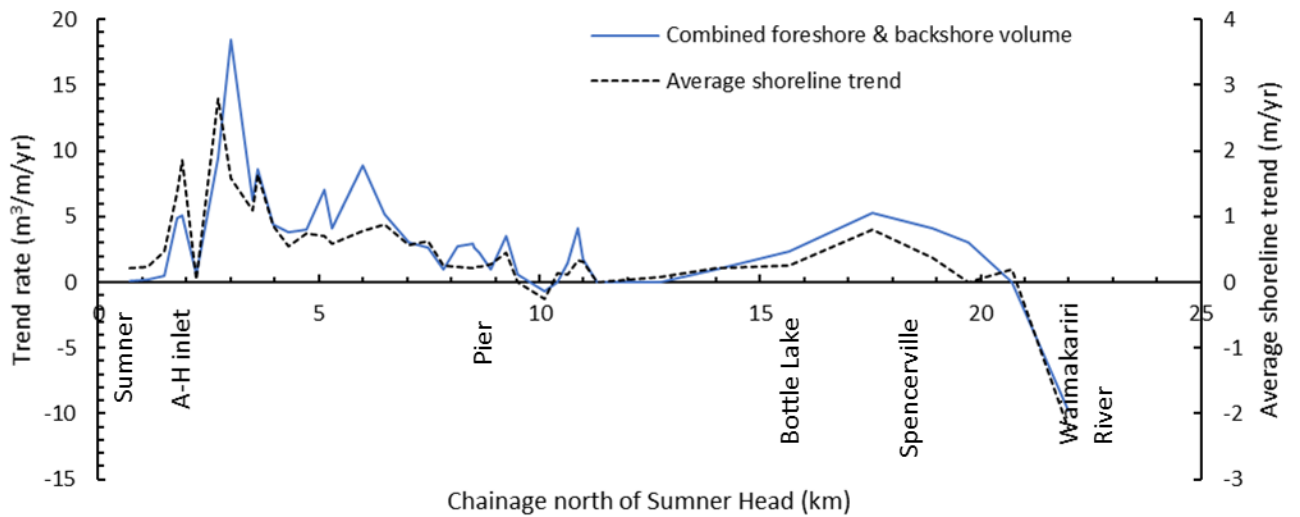


Figure 3-19: Overlay trend rates for upper beach unit volume and average shoreline advance.

3.3.3 Closure depth and lower beach volume changes

Closure depth

We estimated the inner and outer profile closure depths, D_i and D_o , at four locations along the study shore using the time-series output from the SWAN modelling. The results are summarised in Table 3-6. The inner limit ranged from 4.98 to 5.60 m, increasing slightly from south to north by virtue of increasing effective wave height. The outer limit depths ranged from 6.96 to 7.89 m. For our subsequent calculations of outer profile sand accretion, we conservatively adopted the outer limit depth, increasing the value from 7.0 m to 7.9 m northward along the study shore to Spencerville, then keeping it constant at 7.9 m further north.

We note that these values of closure depth are significantly less than those derived by Tonkin & Taylor (2017) for assessing the effects of rising sea level (i.e., 9.5 m from MSL for D_i and 14 m for D_o , respectively). The difference appears to be due to their use of wave statistics recorded at the Banks Peninsula wave buoy, which is in an exposed, deep-water location that experiences higher waves than the study shore.

Table 3-6: Inner and outer profile closure depth estimates derived from Hallermeier's relations with the SWAN-modelled wave records for the period 2000-2017. H_{s-e} is the effective significant wave height; T_s is the matching average peak-energy wave period; H_{s-max} is the maximum significant wave height in the record; D_i is the inner closure depth limit and D_o is the outer limit, as determined with Equations (2) and (3), respectively. Both D_i and D_o have been adjusted to MSL datum by adding 1.0 m.

Wave output station	Location	H_{s-e} (m)	H_{s-max} (m)	T_s (s)	D_i (m)	D_o (m)
50	Southshore	1.92	3.43	8.0	4.98	6.96
61	Parklands	2.07	3.77	8.0	5.24	7.36
68	Spencerville	2.25	3.89	8.0	5.58	7.87
75	Pines Beach	2.26	3.88	8.0	5.60	7.89

Lower beach volumes

To calculate the volume of sand required to be deposited on the lower beach profile to translate it seaward at the average rate of shoreline advance, we multiplied the average rate of advance (as shown in Figure 3-19) by the outer closure depth limit derived above. This produced an inferred lower profile sand accumulation rate of 58,500 m³/yr for the shore between Brooklands Spit and Sumner Beach, or 70,000 m³/yr discounting the eroding profile at the northern tip of Brooklands Spit.

Adding the latter figure to the surveyed accumulation rate on the upper profile (63,000 m³/yr, discounting the erosion at the Brooklands Spit tip) gives an inferred total sand accumulation rate of 133,000 m³/yr.

3.4 Sand exchanges with the Avon-Heathcote tidal deltas and estuary

Effect of Christchurch Earthquake Sequence

Measures et al. (2011) analysed changes in the topography of the Avon-Heathcote Estuary caused by the Christchurch Earthquake Sequence of 2010-2011. They calculated a 14% reduction in the tidal prism of the estuary, and suggested that this might cause the inlet to narrow at Shag Rock and the volume of material stored in the ebb and flood tidal deltas to reduce, thus releasing surplus sand to

nourish the adjacent beaches at Sumner and Southshore. In a subsequent report, Measures and Bind (2013) used 3D hydrodynamic modelling of the estuary to derive a more accurate assessment of the reduction in the spring tidal prism as a result of the earthquake, finding a 12.4% reduction.

Using the empirical equation of Hicks and Hume (1996), Equation (9) in this report, we calculate that a 12.4% reduction in the tidal prism should produce a 16% reduction in the inlet's ebb delta sand volume. Although there is no direct data on the pre-earthquake ebb delta volume, using the Hicks and Hume relation for a free-form ebb delta, Equation (8) herein, with a shore-normal jet and a spring tidal prism of 11.67 million m³ (from Measures and Bind 2013), the estimated pre-earthquake sand volume is 2.92 million m³. Thus, the potential sand release due to the earthquakes is approximately 470,000 m³. If anything, the true original ebb delta volume and its sand losses are likely to be less than these figures because the ebb delta's "accommodation space" is cramped by bedrock outcrops at Shag Rock and Cave Rock (Figure 3-20).

There is no similar information available for changes in the inlet's flood-tide delta, but given the relative small accommodation space available for that, it is reasonable to assume that the reduction in its volume would be small compared to that of the ebb-tide delta and can be ignored.

It is striking that Figure 3-15 shows substantial foreshore accretion adjacent to the Avon Heathcote Inlet from early 2011. We estimate the sand volume in this accretion between chainage 2.2 and 4 km to be approximately 220,000 m³ – which is of similar order to the expected sand transfer off the ebb delta, thus giving substance to the Measures et al. prediction.

Averaged over the 27 years of the profile surveys (1990-2017), this 220,000 m³ figure becomes less significant – averaging approximately 8,100 m³/yr – but it still equates to 12% of the surveyed average accretion rate of the study shore.



Figure 3-20: Ebb-tidal delta seaward of the Avon-Heathcote Inlet. Imagery from Google Earth, dated 2/9/2016.

3.5 Coastal sediment budget

3.5.1 Beach sand 'demand' to meet observed onshore accretion

As discussed above, the 'demand' for beach sand to the study shore not only has to align with the surveyed 1990-2017 average accumulation rates, but it must also include sand to prograde the lower profile. Moreover, sand is also required to lift the profile to balance the rate of sea-level rise.

The need for this sea-level rise component derives from the concepts behind the Bruun model of the response of sandy beaches to rising sea level (see, e.g., Tonkin & Taylor). This requires that (i) the full beach profile rises in pace with sea-level, and (ii) the sand required to lift the lower part of the profile is derived from retreat of the upper profile into the backshore. On an accreting shore like the Christchurch City shore, where backshore erosion does not occur, the sea-level-driven lift in the profile needs to be supplied with sand that would otherwise supply horizontal progradation of the profile.

The required sand supplement for sea-level rise is estimated from the product of the width of the profile (between foredune crest and closure depth), the rate of sea-level rise, and the length of shore. In this study (and following Tonkin & Taylor 2017) we assume a sea-level rise rate of 2 mm/yr. Assuming that the Beatty Street shore profile presented by Allan et al. (1999, Figure 3-21) is reasonably representative of the whole span of study shore, we extracted from that an upper beach width of 100 m and a lower beach width of 800 m out to the closure depth at 7.5 m below MSL.

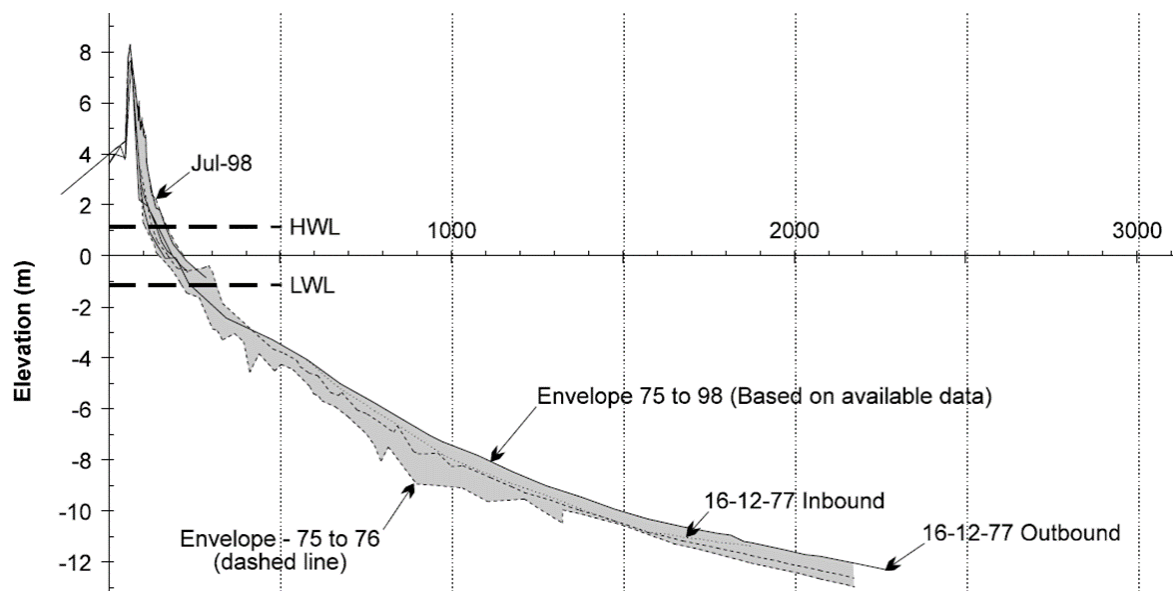


Figure 3-21: Bathymetric profile at Beatty Street, New Brighton. From Allan et al. (1999). Used to estimate the profile width out to the closure depth of around 7.5 m below MSL.

Figure 3-22 shows these various components of the beach sand demand accumulated northward along the study shore from Sumner Beach to chainage 21 km, just south of the Waimakariri River mouth. There is good agreement between the surveyed upper profile sand accumulation (red line) and upper profile accumulation derived from shoreline advance rates and dune height (light blue

line), so we have used the latter for budget totalling. The accumulated totals are: 67,000 m³/yr accreted on the upper profile, a further 70,000 m³/yr predicted to be prograding the lower profile, and 37,000 m³/yr for sea-level rise driven profile lifting, totalling 174,000 m³/yr – which is the sand volume to be matched with potential sand sources.

3.5.2 K-factor calibration

As discussed in Section 3.2.3, we calibrated the *K*-factor in Equation (1) so that the longshore transport potential at chainage 14.8 km matched the accumulated sand ‘demand’ at that point (129,500 m³/yr).

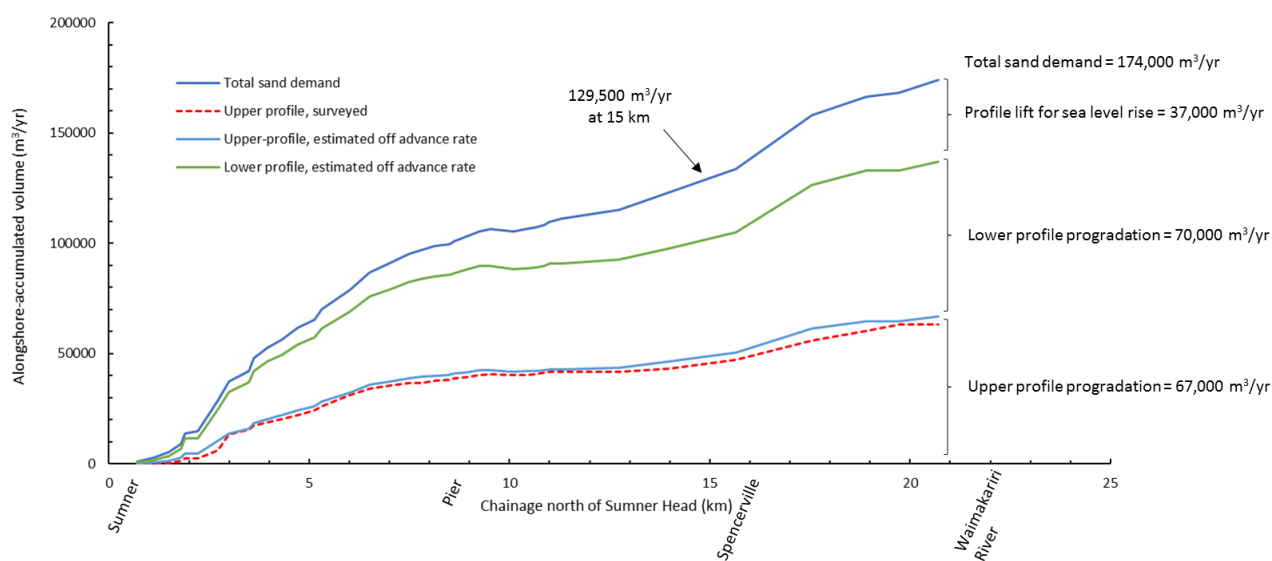


Figure 3-22: Beach volume budget components accumulated and totalled alongshore. Note good agreement between surveyed upper profile sand accumulation (red line) and upper profile accumulation derived from shoreline advance rates and dune height (light blue line). The total sand ‘demand’ at 15 km chainage is used to calibrate the *K*-factor in Equation (1).

3.5.3 Comparing beach sand ‘demand’ with Waimakariri River sand supply

In Section 3.1.5, we concluded that the Waimakariri River discharges 745,000 m³/yr ($\pm 6\%$) over all sand grades to the ocean. In Section 3.1.6, by matching the size-grading of the river’s sand load with that of the beach sand on the study shore, we concluded that only 36% of the river’s total sand discharge would be retained on the active beach profile. Furthermore, in Section 3.2.4, we estimated from the ratio of southward-directed transport potential to gross transport potential around the river mouth that 68% of the river’s sand load would be transported southward towards the Christchurch City shore. Thus, the Waimakariri River’s contribution to the beach sediment budget on the study shore is $745,000 \text{ m}^3/\text{yr} \times 36\% \times 68\% = 182,000 \text{ m}^3/\text{yr}$. This agrees quite well with the beach sand ‘demand’ estimated above (174,000 m³/yr). The misclose is less than the uncertainty due to the standard error of the river load, which equates to $\pm 11,000 \text{ m}^3/\text{yr}$, with further uncertainties relating to the sand trapping efficiency estimates, north/south split of the longshore transport, and the lower profile volume change estimates.

3.5.4 Uncertainties in budget components

Estimated uncertainties in the various components of the beach sand budget, based on estimates of the standard error, are summarised in Table 3-7. When propagating uncertainties, we have assumed

that % errors can be added for terms multiplied together, while the error from summing terms is found by the root-sum-square of the absolute error associated with each term.

Waimakariri River's sand supply

The accumulated uncertainty in the Waimakariri River's net sand discharge is $\pm 15.2\%$. This is sourced reasonably evenly among the estimates of the long-term average load, the sand proportion, and the assumed bulk density. The loss to Brooklands Lagoon, while having a large % error, is so small that it has little impact on the overall uncertainty in the discharge to the coast.

Onshore/offshore split: river sand trap-efficiency on beach profile

The onshore trapping efficiency of the river sand is rendered uncertain by 19% (if anything, the trap efficiency should decrease) by virtue of the lack of size grading data across the full beach profile to closure depth and along the full length of the study shore. A dataset with this information would significantly reduce this uncertainty.

North/south split of river sand

The error in the southward to gross longshore transport ratio stems from the local variability in this ratio observed adjacent to the river mouth from the wave-driven longshore transport analysis. The $\pm 10\%$ error in this ratio was derived from the standard deviation of the ratio at the five SWAN model output stations centred on the river mouth (spanning 2.8 km of shore). It should also be appreciated that the southward/gross ratio is a blunt index of the actual southward/northward split of the Waimakariri River sand because this split is affected by more processes than simply wave-driven surf-zone longshore transport.

River sand delivery to the city beaches

Accumulating the above errors, the uncertainty on the estimated supply of river sand to the city beaches is $\pm 44\%$. As above, the estimate will be higher if the sand trap efficiency has been underestimated. From the above, the best way to reduce this uncertainty level would be through better information on the north/south and onshore/offshore splits of the Waimakariri River sand supply.

Beach sand volume demand

The uncertainty in the beach sand demand accumulates from that of the surveyed upper beach volume gain, the estimated matching progradation of the lower beach profile out to the closure depth, and the sand demand to lift the profile to match sea-level rise. The latter two components dominate the accumulated uncertainty and are controlled by uncertainty in the depth and seaward offset of the closure point, respectively. We have conservatively used the outer Hallermeier depth limit (D_o) to position the closure point; our uncertainty estimates are based on the differences that would result from using Hallermeier's inner limit (D_i). Thus, the beach sand demand may more likely be 16% less than the best estimate.

Longshore transport

Since the longshore transport rates depend on the CERC-formula K -factor, which was calibrated against the long-shore accumulated beach volume demand, we estimate the K -factor uncertainty as $\pm 12\%$ based on the uncertainty in beach sand demand.

Interactions with Avon-Heathcote Inlet system

Based on the observed sand gains adjacent to the Avon-Heathcote Inlet following the Christchurch Earthquake Sequence, permanent sand exchanges between the ebb-tidal delta and the beaches

driven by changes in the estuary’s tidal-prism would appear to be a potentially significant component of the beach sediment budget, but there is considerable uncertainty in the sand volumes involved. We consider this further in the Stage B report when assessing the effects of rising sea-level.

Table 3-7: Estimated uncertainties on the beach sand budget components. A + sign beside the % error indicates that if anything the true value is more likely to be greater than the estimated value; a - sign indicates the reverse; no sign indicates that the true value could equally be greater or less than the estimated value. The error accumulation assumes % errors can be added for terms multiplied together, while the error from summing terms is found by the root-sum-square of the absolute error associated with each term.

Budget component	Estimate	% error
Long-term average SS load (t/yr)	3,030,000	6.5%
Sand equivalent for this load (%)	39.4%	5.6%
Bulk density (t/m ³)	1.6	3.1%
Volumetric sand load to tidal reach (m ³ /yr)	746,000	15.2%
Sand loss to Brooklands Lagoon (m ³ /yr)	1000	50.0%
Net sand load to coast (m³/yr)	745,000	15.2%
Offshore/onshore split (% staying onshore)	36.0%	+19.4%
Longshore split (% moved southward)	68.0%	10%
Total river sand supply to city beaches (m³/yr)	182,000	44.6%
Surveyed sand volume gain - upper beach (m ³ /yr)	67000	3.2%
Estimated sand volume gain - lower beach (m ³ /yr)	70000	-28%
Estimated sand demand for rising sea level (m ³ /yr)	37000	-22%
Total beach sand demand (m³/yr)	170,200	16%

3.5.5 Future monitoring/studies to reduce uncertainties

Recommendation for future monitoring/studies to reduce the above uncertainties include:

- Further gauging and particle-size analysis of the Waimakariri River sediment load - to refine the estimate of river sediment load and address the assumption that the particle size grading determined from high-flow event sampled in January 2018 was representative.
- Comprehensive sampling of grainsize across the outer beach profile along the City shore – to resolve the bulk size grading of the beach sand stock, for comparison with the size grading of the river sand load.
- A study using a numerical model such as XBeach of sand dispersion from the Waimakariri River mouth, including sand transfers seaward of the surf-zone – to better quantify the proportion of the Waimakariri River’s sand load that is distributed south to the City shore.
- Repeat surveys of offshore profile change at a representative selection of ECan’s profiles - to confirm the location of the profile closure depth, and to confirm the

assumption that the inner and outer beach profile segments translate in parallel with long-term-average shoreline shifts.

- Periodic repeat surveys of the Avon-Heathcote inlet and ebb-tidal delta – to confirm the extent of sand exchanges between the inlet system and the adjacent beaches and their impact on shore stability around the inlet.

4 Conclusions

The main conclusions around the contemporary sand budget for the Christchurch City shore are:

- The Waimakariri River is the dominant beach sand source to the city shore, even though only about a quarter of its total sand load appears to be retained on the active beach profile along the city shore.
- Sand removed from the Waimakariri River channel during gravel extraction and at irrigation intakes is a minor fraction of the river's residual sand discharge to Pegasus Bay, and so has minimal impact on the coastal sand budget.
- Sand entrapment in Brooklands Lagoon also has minimal impact on the Waimakariri River's sand discharge.
- The river sand enters a bi-directional longshore transport system, with about 68% estimated to be moving southwards from the Waimakariri River mouth. For about 5-6 km south of the river mouth, processes other than wave-driven surf-zone longshore transport (e.g., transport by the river's discharge jet during floods) appear to be important in moving sand alongshore from the river mouth beyond the surf-zone.
- Away from the river mouth area, wave-driven surf-zone transport would appear to be the dominant process responsible for transporting sand southward and for progressively depositing sand due to a southward-waning transport capacity. Winds blowing along the shore appear to exert only minor influence on the net wave-driven transport, while externally-forced currents (e.g., tidal currents and Canterbury Current eddies) also appear to have minor net impact.
- The city shore is accreting along most of its length, and the sand 'demand' to sustain this accretion must also prograde the lower beach profile, seaward of the MSL line out to the closure depth, as well as lift the beach profile to keep pace with rising sea-level. This total 'demand' for beach sand is more than twice the volume surveyed to be accumulating above the MSL line.
- Our estimate of this beach sand demand aligns reasonably well with our estimates of the supply of Waimakariri River sand to the city beaches. The sand budget misclose between supply and demand is well within the uncertainties accumulated from the various budget components.
- There is circumstantial evidence in the ECan beach profile dataset that the Canterbury Earthquake Sequence, by altering the topography of the Avon Heathcote Estuary and reducing its tidal prism, caused the estuary's ebb tidal delta to shrink, thus releasing sand to the adjacent beaches.

5 Acknowledgements

We thank:

- Fiona Crombie (Central Plains Water Ltd), Paul Reese (Irricon), Brent Walton (Waimakariri Irrigation Ltd) and Daniel Meehan (Selwyn District Council) for discussing the operation and design of the main surface water takes from the Waimakariri River.
- Bruce Gabites (ECan) for supplying ECan's beach profile dataset for southern Pegasus Bay.
- Justin Cope (ECan) for supplying ECan's 1997 dataset on beach sand size gradings and providing feedback on the draft report.
- Hamish Sutton, Marty Flanagan, Jeremy Rutherford, and Alec Dempster (all from NIWA) for undertaking the lower Waimakariri River suspended sediment and bed-material sampling.
- Paul Lambert (NIWA) for the sediment sample laboratory analysis.
- Shaun McCracken (ECan) for supplying updated data on Waimakariri River gravel extraction.
- Bas van Lammeren, John Walter, and Marion Schoenfeld from Christchurch City Council for providing feedback on the draft report.

6 References

- Allan, J.C., Kirk, R.M., Hemmingsen, M., Hart, D. (1999) Coastal processes in Southern Pegasus Bay: A review. A Report to Woodward-Clyde New Zealand Limited and the Christchurch City Council, prepared by Land and Water Studies (International) Ltd, Christchurch, June 1999.
- Blake, G.J. (1968) The rivers and the foreshore sediment of Pegasus Bay, South Island, New Zealand, *New Zealand Journal of Geology and Geophysics*, 11:1, 225-235, DOI: 10.1080/00288306.1968.10423687
- Bolton-Ritchie, L. (2007). Sediments and benthic macrobiota of Brooklands Lagoon. Report No. U07/52. Environment Canterbury.
- Booij, N., Ris, R.C., Holthuijsen, L.H. (1999) A third-generation wave model for coastal regions. 1. Model description and validation. *Journal of Geophysical Research* 104(C4): 7649-7666.
- Bruun, P. (1954) Coastal erosion and the development of beach profiles. Technical Memorandum No.44, Beach Erosion Board.
- Bruun, P. (1962) Sea level rise as a cause of shore erosion. *Journal of Waterway, Port, Coastal and Ocean Engineering*, American Society of Civil Engineers, 88, 117-130.
- Campbell, J.R. (1974) Processes of littoral and nearshore sedimentation in Pegasus Bay. Unpublished M.A thesis, in Geography, University of Canterbury, N.Z. 97pp.
- Carter, L., Herzer, R.H. (1986) Pegasus sediments. 2nd Ed., New Zealand Oceanographic Institute Chart, Coastal Series, 1: 200,000.
- CERC (1984) Shore protection manual. Vols I and II. Coastal Engineering Research Center, US Army Corps of Engineers, Vicksburg, Mississippi.
- Dean, R. G. (1991) Equilibrium beach profiles: characteristics and applications. *Journal of Coastal Research*, 7(1), 53–84. <https://doi.org/10.2307/4297805>
- Christchurch City Council (2010) Brooklands Lagoon / Te Riu O Te Aika Kawa area: Parks Master Plan, August 2010.
- Gabites, B. (2005) A summary of monitoring and investigations on the Pegasus Bay coastline, 1998-2005. Environment Canterbury Technical Report No U06143.
- Gorman, R., Hicks, M., Walsh, J. (2002) Canterbury open-coast wave refraction and longshore transport study. *NIWA Client Report ENC02509* prepared for Environment Canterbury, June 2002.
- Hicks, D.M. (1993) Modelling long-term change of the Pegasus Bay shoreline. Miscellaneous Report No. 99, Report to the Canterbury Regional Council, NIWA, Christchurch, July 1993.
- Hicks, D. M., Duncan, M. J. (1993) Sedimentation in the Styx River Catchment and Brooklands Lagoon. Report to the Christchurch City Council and Environment Canterbury. Miscellaneous Report No. 128. Freshwater Division, NIWA, Christchurch.

- Hicks, D.M., Hume, T.M. (1996) Morphology and size of ebb tidal deltas at natural inlets on open-sea and pocket-bay coasts, North Island, New Zealand. *Journal of Coastal Research* 12(1): 47-63.
- Holmquist-Johnson, C.L., Raff, D. (2006) Bureau of Reclamation Automated Modified Einstein Procedure (BORAMEP) program for computing total sediment load. Federal Interagency Sedimentation Conference in Reno, NV., April 2-6, 2006. Federal Interagency Sedimentation Project. p. 8.
- McConnell Dowell (2007) Christchurch City Council Ocean Outfall Pipeline Project Construction Execution Procedure for Wave Buoy Installation, Project No. 2902, Document No. V009-600-2902.
- Measures, R. J., Hicks, D.M., Shankar, U., Bind, J., Arnold, J., Zeldis, J. (2011) Mapping earthquake induced topographical change and liquefaction in the Avon-Heathcote Estuary. *NIWA Client Report* Prepared for Environment Canterbury. ECan Report No. U11/13. ISBN 978-1-927195-90-1.
- Measures, R.J. (2012) Modelling gravel transport, extraction and bed level change in the Waimakariri River, *NIWA Client Report* CHC2012-121. Prepared for Environment Canterbury.
- Measures R.J., Bind J. (2013) Hydrodynamic model of the Avon Heathcote Estuary: Model build and calibration, *NIWA Client Report* CHC2013-116.
- Nicholls, R.J., Laron, M., Capobianco, M., Birkemeier, W.A. (1998) Depth of Closure: Improving understanding and prediction. ICCE 1998.
- Ris, R.C., Holthuijsen, L.H., Booij, N. (1999) A third-generation wave model for coastal regions. 2. Verification. *Journal of Geophysical Research* 104(C4): 7667-7681.
- Soulsby, R.L. (1997) *Dynamics of marine sands*. Thomas Telford Publications, London, ISBN 07272584X.
- Stephen, G.D., Nottage, D. A. (1959) Waimakariri River - Analysis of coarse bed materials, North Canterbury Catchment Board.
- Tonkin & Taylor (2017) Coastal hazard assessment for Christchurch and Banks Peninsula. Prepared for Christchurch City Council by Tonkin & Taylor Ltd, October 2017.
- van Rijn, L.C. (1985) Sediment transport, part III: bed forms and alluvial roughness. *Journal of Hydraulic Engineering*, 110(12):1733–1754.

Appendix A Wave refraction modelling and longshore transport calculation

SWAN model

Wave conditions along the project coast were simulated using the SWAN (Simulating Waves Nearshore model - Booij et al. 1999; Ris et al. 1999). This is a spectral model in that it describes the sea state in terms of the wave spectrum $S(f, \theta)$, representing the amount of energy associated with waves in each band of wave frequency f and propagation direction θ . The model computes the evolution of this wave spectrum by accounting for the input, transfer and loss of energy through the various physical processes acting on waves in shallow water. These include the effects of refraction by currents and bottom variation, and the processes of wind generation, white-capping, bottom friction, quadruplet wave-wave interactions, triad wave-wave interactions and depth-induced breaking.

Model domain

A model grid was established covering the South Island east coast north of the Otago Peninsula, and terminating at the southern end of the North Island, oriented at 40° from True North to align with the trend of the coastline. The wave model was run at 1000 m resolution on a regular grid of 117 cells in the cross-shore direction by 631 cells in the longshore direction. The grid origin (cell (1,1)) was at NZMG (2255650.0E, 5525000.0N). The spectral grid had 25 discrete frequencies logarithmically placed between 0.0418 Hz and 0.802 Hz, and 32 direction bins at 11.25° increments.

Simulation period

A simulation was run from September 2000 through December 2017.

Inshore wind field

The model was forced with a spatially-uniform wind field which altered the wave field between that measured at the buoy and as refracted to the shore. The wind field forcing was derived from measured wind records from Brighton Pier at times when those data were available. Gaps in the record were infilled using wind records from Christchurch Airport, rescaled using a linear regression

$$V_{BP} = 0.92 V_{CA} + 1.28 \quad (1)$$

obtained from the ~ 5 years of overlapping wind speed data (10 Oct 2011 – 24 Aug 2016) at the two sites, where V_{BP} and V_{CA} are the wind speed at Brighton Pier and Christchurch airport, respectively.

Wave buoy boundary condition

The SWAN model can incorporate boundary conditions representing waves arriving from outside the model domain. For this study, wave boundary conditions were derived from data recorded by the Banks Peninsula Directional Waverider, located at (43.7567°S, 173.3358°E). This instrument records accelerations in three dimensions, for 20-minute bursts at 1.28 Hz sampling frequency. Since October 2004, these bursts have been recorded at 30-minute intervals, but earlier records were at hourly or three-hourly intervals. The burst records are processed to derive averaged frequency spectra from 8 blocks of 256 samples each, giving co- and cross-spectra between the three (x, y and z) components of the displacement signal at 0.005 Hz frequency resolution.

The buoy record does not fully characterise the directional dependence of the wave spectrum, but provides estimates of the mean direction and directional spread at each frequency, which we then use to provide a directional spectrum of the form

$$S(f, \theta) = S(f)[(\theta - \theta_0(f))/2]^{p(f)} \quad (2)$$

as boundary conditions for the model, along the full offshore boundary.

The buoy site is exposed to persistent southerly swells, which are largely blocked by Banks Peninsula from reaching the Pegasus Bay coast. On the other hand, waves from the eastern quadrant have a relatively stronger impact at the coast than at the buoy location. Being more locally-generated, these will generally occur in the buoy record at higher frequencies than the southerly swell. Where both are present simultaneously, the above formulation will allow for both components of the sea state to be satisfactorily represented. In the Gorman et al. (2002) study, by contrast, it was only possible to apply parametric boundary conditions, specifying a single mean direction and directional spread to apply to all frequencies. Hence only one component could be represented at a time, meaning that the role of waves reaching Pegasus Bay from the northeast could often be under-represented relative to those from the southeast.

SWAN model outputs at 10 m isobath stations

SWAN model output was extracted at stations located approximately 700-800 m apart along the 10-m isobath along the study shore and also extending north beyond Amberley at the northern end of Pegasus Bay and south around Banks Peninsula (in order to provide a broader perspective on wave energy patterns).

As well as common wave statistics such as the significant wave height we also calculated H_{m0} :

$$H_{m0} = 4\sqrt{M_0} \quad (3)$$

where

$$M_0 = \iint S(f, \theta) df d\theta \quad (4)$$

these model outputs also included the energy transport, (i.e., the energy crossing unit length of wave front per unit time),

$$\vec{F} = \iint 2\rho g \vec{C}_g(f, \theta) S(f, \theta) df d\theta \quad (5)$$

where $\vec{C}_g(f, \theta)$ is the (vector) group velocity of each component, $\rho = 1025 \text{ kg/m}^3$ is the density of seawater and $g = 9.81 \text{ m/s}^2$ is the gravitational acceleration.

We can take its longshore and onshore components

$$F_{LS} = \vec{F} \cdot \vec{n} = |\vec{F}| \sin \alpha \quad (6)$$

and

$$F_{OS} = |\vec{F}| \cos \alpha \quad (7)$$

where \vec{n} is the (shoreward-pointing) unit normal vector to the isobath, and α is the relative angle between the mean wave flux direction and the shoreward normal, at the 10-m isobath.

The longshore flux per unit length of beach is

$$P_{LS} = F_{LS} \cos \alpha \quad (8)$$

The energy transport is a conserved quantity until depth-induced breaking commences, so we assume that its magnitude F_b at the breakpoint is the same as at the 10-m isobath. Also, for shallow water of depth h , the group velocity has magnitude

$$C_g \approx \sqrt{gh} \quad (9)$$

so, we can estimate the wave energy flux at the breakpoint

$$F_b = \frac{1}{8} \rho g C_g H_b^2 = F_{10} \quad (10)$$

Assuming further that the wave height on breaking is proportional to the depth, i.e.,

$$H_b \approx \gamma h_b \quad (11)$$

with a constant of proportionality $\gamma \approx 0.5$. Hence the (conserved) magnitude of the energy transport at both the 10-m isobath and at the breakpoint is

$$F_b = F \approx \frac{\rho g^{1.5}}{8\gamma^{0.5}} H_b^{2.5} \quad (12)$$

Conservation of the longshore component of wavenumber gives (Snell's law):

$$\sin \alpha_b / \sin \alpha = \frac{k}{k_b} \approx \sqrt{\frac{h_b}{h}} \quad (13)$$

where α and α_b are the angles between the wave propagation direction and the shore-normal direction at the 10-m isobath and at the breakpoint, respectively, and $h = 10$ m and h_b are the corresponding depths. Equivalently, the wave crests are at an angle α_b to the beach.

The energy transport at the breakpoint has longshore and onshore components $F \sin \alpha_b$ and $F \cos \alpha_b$ respectively. The flux of longshore directed wave energy across a shore-parallel line is then given by the "longshore flux factor"

$$P_{ls} = F \cos \alpha_b \sin \alpha_b = \frac{1}{2} F \sin 2\alpha_b \approx \frac{\rho g^{1.5}}{16\gamma^{0.5}} H_b^{2.5} \sin 2\alpha_b \quad (14)$$

while the flux of onshore-directed wave energy across a shore-parallel line is

$$P_{os} = F \cos^2 \alpha_b \approx \frac{\rho g^{1.5}}{16\gamma^{0.5}} H_b^{2.5} \cos^2 \alpha_b \quad (15)$$

Longshore transport

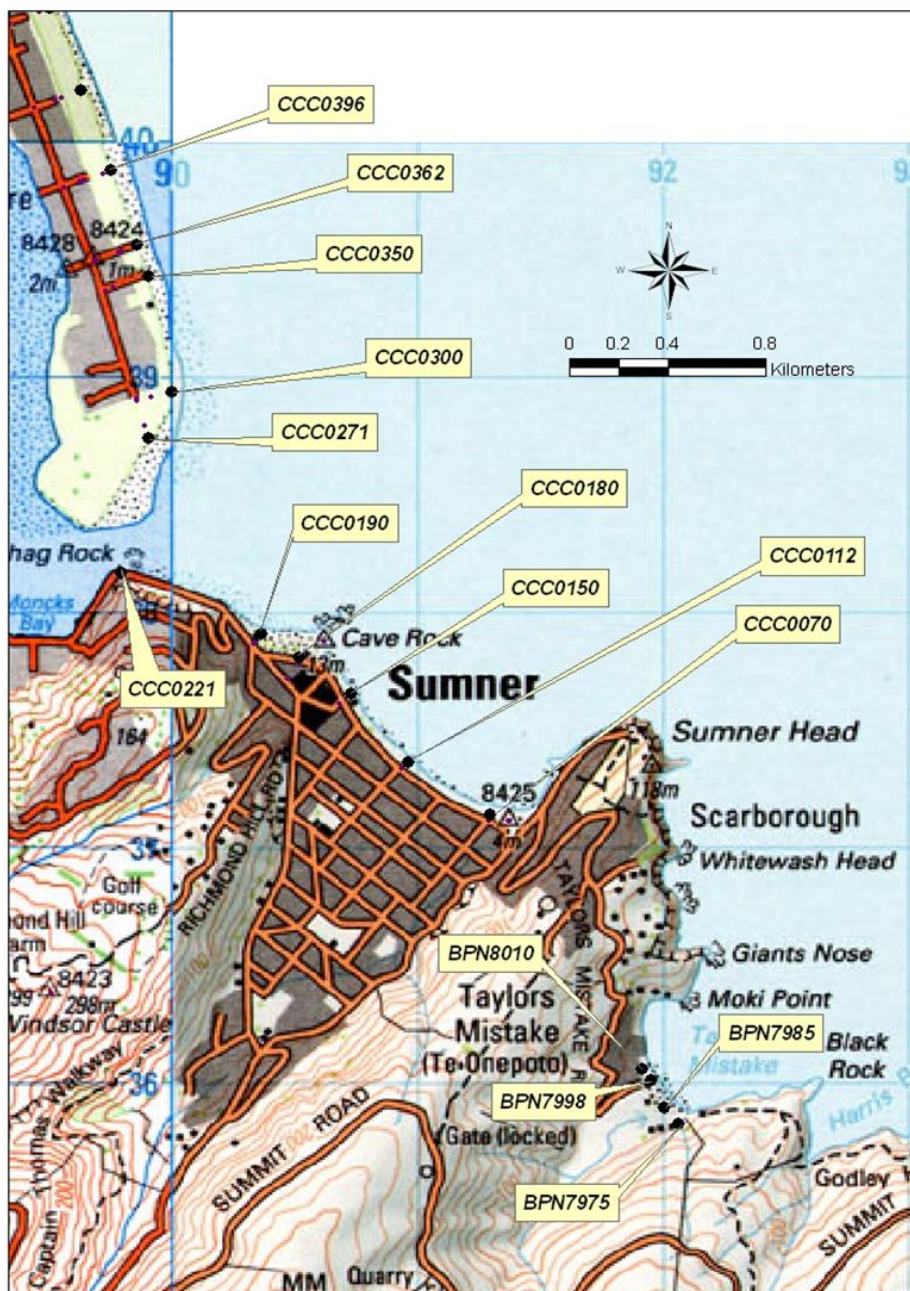
The longshore sediment flux can be approximated from P_{ls} by an empirical relationship (CERC 1984)

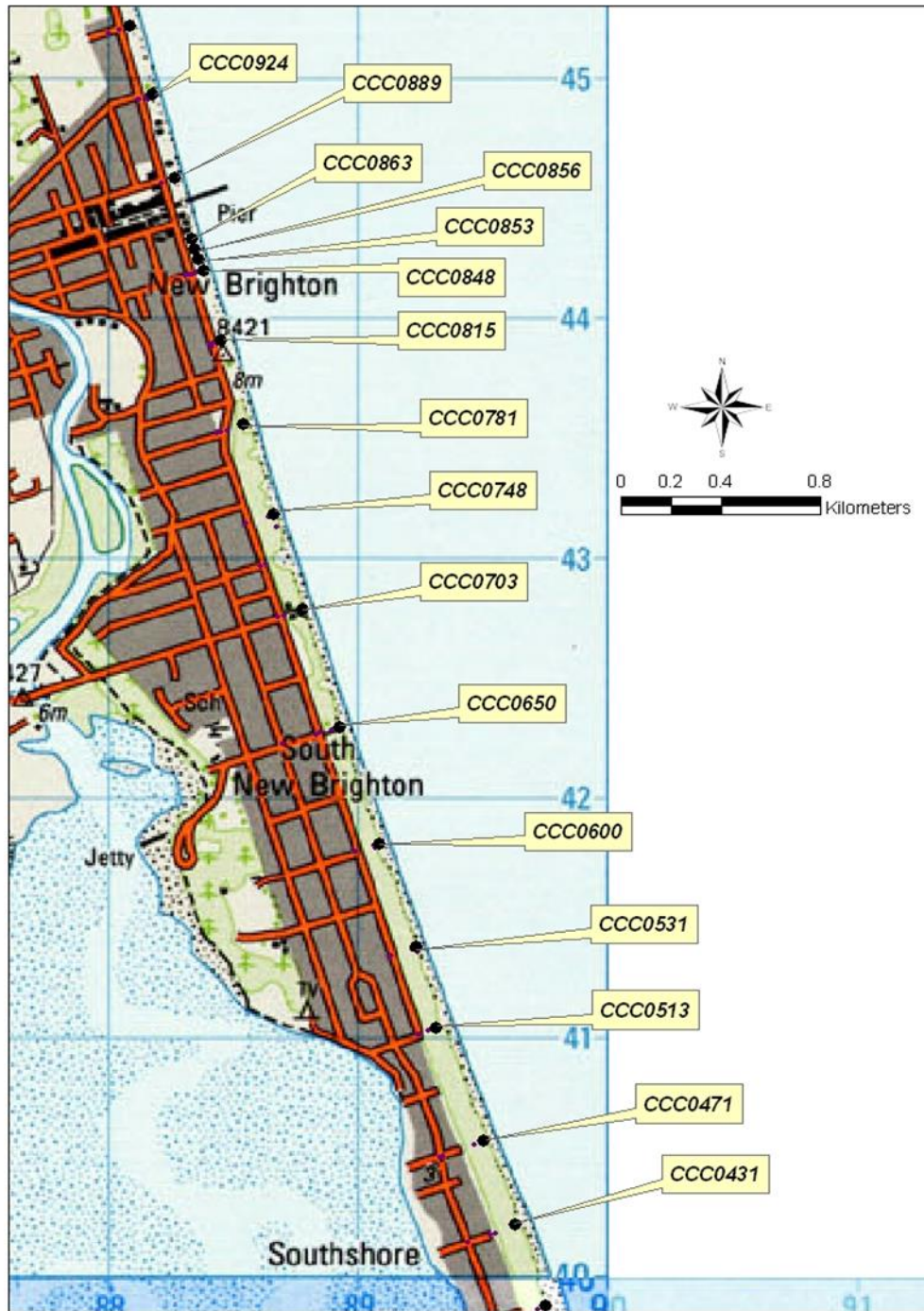
$$Q = f K P_{ls} \quad (16)$$

where $f = 3249 \text{ m}^2\text{s}^3/\text{kg}/\text{yr} = 1.05 \times 10^{-4} \text{ m}^2\text{s}^2/\text{kg}$ is a unit-conversion constant, while K is a dimensionless efficiency factor dependent on sediment properties. For this study, northward transport was deemed to be positive.

Appendix B ECan beach profile locations

The Environment Canterbury beach profiles are located on the following maps from Gabites (2005). Note that the profile naming conventions for the Christchurch City shore profiles includes the chainage north from Sumner Head prefixed by CCC (e.g., Profile CCC0271 is located 2.71 km north from Sumner Head). The profiles at Taylors Mistake (prefixed with "BPN") are named off the chainage north from the southern side of Banks Peninsula (e.g., Profile BPN8010 is located 80.1 km north north around the coast of Banks Peninsula). For convenience with this study, the Taylors Mistake profiles have also been assigned a (negative) chainage north of Sumner Head, assuming that profile BPN8010 is at chainage -1.6 km.









Appendix C Starting offsets used in beach volume calculations

Starting offsets for the calculations of beach volume change were set to manage inconsistencies in the landward extent of the ECan profile surveys. The surveyed extents of profiles varied due to the field surveyor judging that the backshore profile had not changed significantly since the previous full backshore survey. For most profiles a reliable end-point that fully captured the change in backshore volume over time could be assigned. However, some profiles had sparse data in the backshore that required an end-point to be assigned that was further seaward than ideal to avoid spurious inter-survey volume changes. Table C-1 lists the offsets to the volume-calculation end-points selected for each profile, and identifies and comments on those profiles where the backshore volume changes may be less reliable.

Table C-1: Offsets to start of beach volume calculation for ECan profiles and assessments of volume change reliability.

Profile	Offset at start of beach volume calculation (m)	Backshore beach volume change adequately represented?	Comments
BPN7975	0.0	Y	
BPN7985	100.0	Y	
BPN7998	2.7	N	Backshore poorly resolved; recent surveys don't cover 0-2.7 m.
BPN8010	0.0	Y	
CCC0070	47.5	NA	No foredune.
CCC0112	40.0	NA	No foredune.
CCC0150	75.0	NA	No foredune.
CCC0180	24.3	Y	
CCC0190	0.0	Y	Backfilled surveys to X=0.
CCC0221	11.0	Y	
CCC0271	210.0	N	Volume change is calculated to the crest of the foredune. Beyond this, the backshore survey data is poorly resolved.
CCC0300	140.0	N	Volume change is calculated to the landward toe of the foredune. The backshore profile landward of this is not well captured in the survey.
CCC0350	182.3	N	Volume change is calculated to the crest of the foredune. The backshore profile landward of this is not surveyed but is assumed to be stable.
CCC0362	144.3	Y	Foredune well represented.
CCC0396	200.0	N	Foredune well represented. Backshore landward of this is not. Volume change is calculated to the crest of the foredune. Some volume change may have been missed.
CCC0431	200.0	N	Foredune well represented. Backshore landward of this is not. Volume change is calculated to the crest of the foredune. Some volume change may have been missed.
CCC0471	184.0	N	Foredune well represented. Backshore landward of this is not. Volume change is calculated to the back of the foredune. Some volume change may have been missed.
CCC0513	0.0	Y	Merged data into survey 12/5/1995. Good data from x=0.

Profile	Offset at start of beach volume calculation (m)	Backshore beach volume change adequately represented?	Comments
CCC0531	80.0	Y	Merged data into surveys. Volume change calculated to just landward of the foredune crest. Ignoring two surveys that look incorrect, profiles landward of this point appear relatively stable suggesting that no significant volume change has been missed
CCC0600	12.0	Y	Merged data into surveys.
CCC0650	50.0	Y	Merged data into surveys. Good data from x=50.
CCC0703	92.0	Y	Good data from x=92.
CCC0748	95.0	Y	Good data from x=95.
CCC0781	75.0	Y	Some minor sand volume change was missed on the landward side of the foredune to avoid poorly resolved survey data.
CCC0815	0.0	Y	
CCC0848	13.0	Y	
CCC0853	53.0	Y	
CCC0856	0.0	Y	
CCC0863	28.5	Y	
CCC0889	60.0	Y	
CCC0924	15.0	Y	
CCC0952	40.0	N	Volume change is calculated to the foredune crest. Survey data in the backshore landward of the foredune crest is inadequately defined. Significant volume change is shown but may be erroneous.
CCC1011	0.4	Y	
CCC1041	14.0	Y	
CCC1065	18.1	Y	
CCC1086	30.0	Y	
CCC1100	15.7	Y	
CCC1130	30.0	Y	Volume change is calculated to just landward of the foredune crest. Only minor volume change is missed in the backshore profile further landward.
CCC1273	0.0	Y	Volume change is calculated to the crest of the second dune in the dune field. The backshore profile further landward is mostly stable.
CCC1400	0.0	N	Volume change is calculated to the foredune crest. Some volume change backshore of this is apparent. Missing data has prevented this being included.
CCC1565	-10.0	Y	Volume change is calculated to just landward of the foredune crest. The backshore profile further landward appears to be stable.
CCC1755	0.0	Y	Volume change is calculated to the foredune crest. The backshore profile further landward appears to be stable.
CCC1891	33.4	Y	Volume change is calculated to the crest of the second dune in the dune field. The backshore profile further landward is mostly stable.
CCC1972	24.0	Y	
CCC2070	91.0	Y	Volume change is calculated to just landward of the foredune crest. The backshore profile further landward appears to be stable.

Profile	Offset at start of beach volume calculation (m)	Backshore beach volume change adequately represented?	Comments
CCC2200	-7.8	Y	Volume change is calculated to just landward of the foredune crest. The backshore profile further landward appears to be stable.